

New Journal of chemistry

Supporting Information

Synthesis and biological evaluation of new fluconazole β -lactam conjugates linked via 1,2,3-triazole

Jaisingh M. Divse,^a Santosh B. Mhaske,^a Chaitanya R. Charolkar,^a Duhita T. sant,^b Mukund V. Deshpande,^b Vijay M. Khedkar,^{c,d} Laxman U. Nawale,^e Dhiman Sarkar,^e and Vandana S. Pore*^a

^a Organic Chemistry Division, CSIR-National Chemical Laboratory, Pune 411008, India.

^b Biochemical Sciences Division, CSIR-National Chemical Laboratory, Pune 411008, India.

^c School of Health Sciences, University of KwaZulu Natal, Westville Campus, Durban 4000, South Africa.

^d Department of Pharmaceutical Chemistry, St. John Institute of Pharmacy & Research, Palghar (E) 401404, India.

^e Combichem-Bioresource Center, Organic Chemistry Division, CSIR-National Chemical Laboratory, Pune 411008, India.

Table of Contents

General procedure for synthesis of imines 6(a-l).....	2-5
General procedure for the synthesis of β -lactams 7,8(a-l).....	5-8
Table 1S.....	8
Molecular docking of compounds 12(a-l).....	9
Table 2S.....	11
Fig 1S-14S.....	16-21
MTT assay.....	21
^1H , ^{13}C -NMR and HRMS data	22-46
HPLC data of compound 12j	47
References.....	48

Supporting Information

Synthesis and biological evaluation of new fluconazole β -lactam conjugates linked via 1,2,3-triazole

Jaisingh M. Divse,^a Santosh B. Mhaske,^a Chaitanya R. Charolkar,^a Duhita T. sant,^b Mukund V. Deshpande,^b Vijay M. Khedkar^{c,d} Laxman U. Nawale,^c Dhiman Sarkar,^c and Vandana S. Pore*^a

^a Organic Chemistry Division, CSIR-National Chemical Laboratory, Pune 411008, India.

^b Biochemical Sciences Division, CSIR-National Chemical Laboratory, Pune 411008, India.

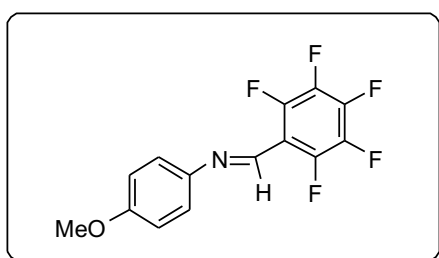
^c CombiChem-Bioresource Center, Organic Chemistry Division, CSIR-National Chemical Laboratory, Pune 411008, India.

^d School of Health Sciences, University of KwaZulu Natal, Westville Campus, Durban 4000, South Africa.

General procedure for synthesis of Imines (6a-l)

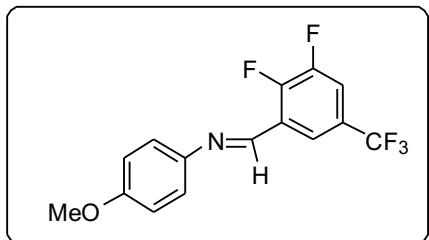
Amine (1mmol), and aldehyde (1-1.2mmol) was taken in a conical flask and kept it inside ordinary domestic microwave oven for 5-8 mins under 540 W. The conical flask was removed out and kept for 15-20 mins at room temperature. The reaction mixture in liquid form was slowly became solid. The solid obtained was then first washed with pet ether and then by 5:95 ethyl acetate: pet ether solution. The solid was obtained in high yeilds (80-98%) and used further without any purification.

(E)-N-(4-methoxyphenyl)-1-(perfluorophenyl) methanimine (6a)



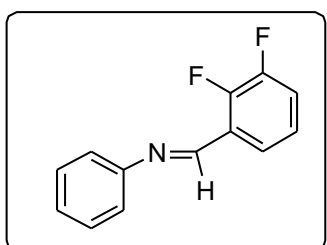
Yield: 92%; M.P 122-123 °C; IR (CHCl₃, cm⁻¹) 1617, 3019; ¹H NMR (CDCl₃, 200 MHz) δ 8.50 (S, 1H), 7.64-7.71 (m, 1H), 7.45-7.52 (m, 1H), 7.19-7.31 (m, 1H), 6.94-7.0 (m, 1H), 3.88 (s, 3H); ¹³C NMR (CDCl₃, 50 MHz) δ 165.5, 160.6, 158.5, 156.6, 144.2, 138.8, 130.2, 124.7, 122.2, 114.6, 55.45. ESI-MS (m/z): 302.14[M+H]⁺.

(E)-1-(2,3-difluoro-5-(trifluoromethyl)phenyl)-N-(4-methoxyphenyl)methanimine (6b)



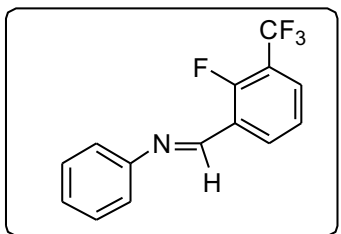
Yield: 89%; M.P 58-59 °C; IR (CHCl₃, cm⁻¹) 1617, 3019; ¹H NMR (CDCl₃, 200 MHz) δ 8.78 (s, 1H), 8.42 (dd, J = 5.56 Hz, 1H), 7.75 (dd, J = 6.44 1H), 7.30-7.35 (m, 2H), 6.94-6.99 (m, 2H), 3.86 (s, 3H); ¹³C NMR (CDCl₃, 50 MHz) δ 162.0, 159.3, 156.9, 147.9, 143.4, 129.2, 123.5, 122.7, 120.2, 114.5, 55.5; ESI-MS (m/z): 316.24[M+H]⁺.

(E)-1-(2,3-difluorophenyl)-N-phenylmethanimine (6c)



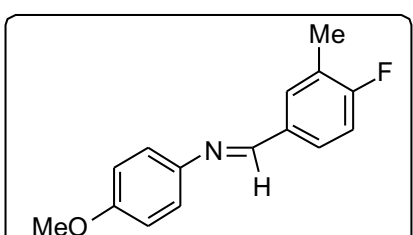
Yield: 80%; sticky solid; IR (CHCl₃, cm⁻¹) 1617, 3019; ¹H NMR (CDCl₃, 200 MHz) δ 8.65 (s, 1H), 7.80-7.87 (m, 1H), 7.28-7.35(m, 1H), 7.04-7.26 (m, 6H); ¹³C NMR (CDCl₃, 50 MHz) δ 153.1, 152.1, 151.3, 148.4, 146.2, 129.2, 126.6, 122.5, 120.9, 118.5, 115.0; ESI-MS (m/z): 218.24[M+H]⁺.

(E)-1-(2-fluoro-3-(trifluoromethyl)phenyl)-N-phenylmethanimine (6d)



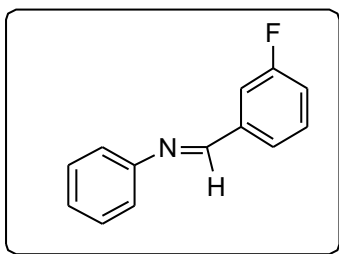
Yield: 75%; sticky solid; IR (CHCl₃, cm⁻¹) 1617, 3019; ¹H NMR (CDCl₃, 400 MHz) δ 8.82 (s, 1H), 8.44 (t, J= 7.34 Hz, 1H), 7.75 (t, J= 7.34 Hz, 1H), 7.43-7.47 (m, 2H), 7.35-7.39 (m, 1H), 7.28-7.31 (m, 3H); ¹³C NMR (CDCl₃, 50 MHz) δ 151.6, 151.2, 131.8, 129.2, 126.8, 125.3, 124.2, 123.7, 120.9; ESI-MS (m/z): 268.08[M+H]⁺.

(E)-1-(4-fluoro-3-methylphenyl)-N-(4-methoxyphenyl)methanimine (6e)



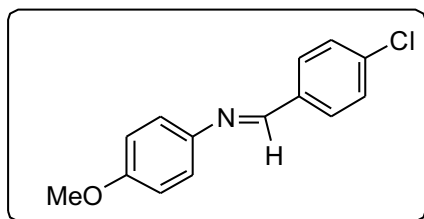
Yield: 93%; M.P 74-75 °C; IR (CHCl₃, cm⁻¹) 1617, 3019; ¹H NMR (CDCl₃, 200 MHz) δ 8.46 (s, 1H), 7.68-7.86 (m, 2H), 7.25-7.30 (m, 2H), 7.12-7.18 (m, 1H), 6.97-7.01 (m, 2H), 3.89 (s, 1H), 2.39 (s, 3H); ¹³C NMR (CDCl₃, 50 MHz) δ 190.7, 165.5, 160.6, 158.2, 157.2, 144.6, 132.3, 131.4, 131.3, 128.2, 125.3, 122.0, 115.5, 114.3, 55.4, 14.4; ESI-MS (m/z): 244.28[M+H]⁺.

(E)-1-(3-fluorophenyl)-N-phenylmethanimine (6f)



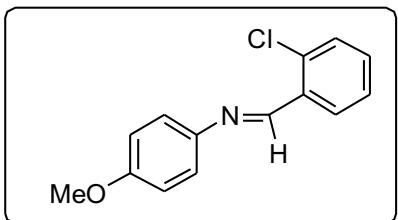
Yield: 88%; sticky solid; IR (CHCl₃, cm⁻¹) 1617, 3019; ¹H NMR (CDCl₃, 400 MHz) δ 8.48 (s, 1H), 7.66-7.73 (m, 2H), 7.43-7.51 (m, 3H), 7.18-7.32 (m, 4H); ¹³C NMR (CDCl₃, 50 MHz) δ 165.5, 160.6, 158.8, 151.4, 138.5, 138.4, 130.3, 129.1, 126.2, 120.8, 118.5, 115.1; ESI-MS (m/z): 200.08[M+H]⁺.

(E)-1-(4-chlorophenyl)-N-(4-methoxyphenyl)methanimine (6g)



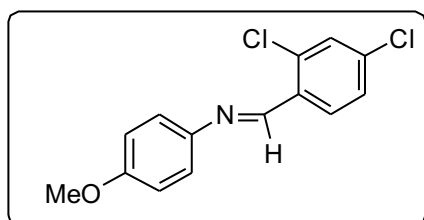
Yield: 98%; M.P 115-116 °C; IR (CHCl₃, cm⁻¹) 1617, 3019; ¹H NMR (CDCl₃, 200 MHz) δ 8.49 (s, 1H), 7.88 (d, J = 8.46 Hz, 2H), 7.49 (d, J = 8.46, 2H), 7.29 (d, J = 8.84, 2H), 6.99 (d, J = 6.69, 2H), 3.89 (s, 3H); ¹³C NMR (CDCl₃, 50 MHz) δ 158.4, 156.5, 144.2, 136.8, 134.8, 129.6, 128.9, 122.1, 114.3, 55.3; ESI-MS (m/z): 246.08[M+H]⁺.

(E)-1-(2-chlorophenyl)-N-(4-methoxyphenyl)methanimine (6h)



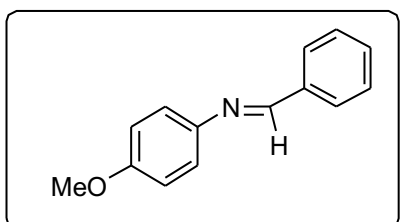
Yield: 98%; M.P 56-57°C; IR (CHCl₃, cm⁻¹) 1617, 3019; ¹H NMR (CDCl₃, 200 MHz) δ 8.95 (s, 1H), 8.22-8.26 (m, 1H), 7.27-7.41 (m, 5H), 6.93-6.98 (m, 2H), 3.85 (s, 3H); ¹³C NMR (CDCl₃, 50 MHz) δ 158.5, 154.6, 144.4, 135.7, 131.7, 129.8, 128.2, 122.4, 114.3, 55.4; ESI-MS (m/z): 246.08[M+H]⁺.

(E)-1-(2,4-dichlorophenyl)-N-(4-methoxyphenyl)methanimine (6i)



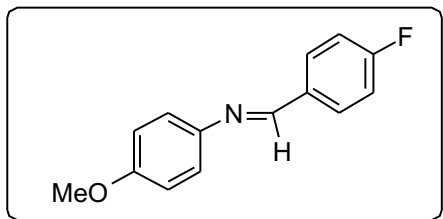
Yield: 96%; M.P 94-95°C; IR (CHCl₃, cm⁻¹) 1617, 3019; ¹H NMR (CDCl₃, 200 MHz) δ 8.88 (s, 1H), 8.20 (d, J = 8.46 Hz, 1H), 7.45 (d, J = 2.02Hz, 1H), 7.27-7.37 (m, 3H), 6.94-6.98 (m, 2H), 3.86(s, 3H); ¹³C NMR (CDCl₃, 50 MHz) δ 158.8, 153.1, 144.1, 137.0, 136.1, 132.0, 129.5, 129.1, 122.5, 114.4, 55.4; ESI-MS (m/z): 280.04[M+H]⁺.

(E)-N-(4-methoxyphenyl)-1-phenylmethanimine (6j)



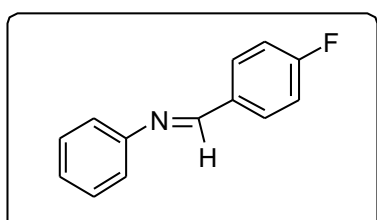
Yield: 98%; M.P 70-71 °C; IR (CHCl₃, cm⁻¹) 1617, 3019; ¹H NMR (CDCl₃, 200 MHz) δ 8.48 (s, 1H), 7.86-7.91 (m, 2H), 7.44-7.49 (m, 3H), 7.20-7.26 (m, 2H), 6.89-6.97 (m, 2H), 3.83 (s, 3H); ¹³C NMR (CDCl₃, 50 MHz) δ 158.2, 158.1, 144.7, 136.3, 130.9, 128.6, 122.1, 114.2, 55.3; ESI-MS (m/z): 212.08[M+H]⁺.

(E)-1-(4-fluorophenyl)-N-(4-methoxyphenyl)methanimine (6k)



Yield: 97%; M.P 86-87 °C; IR (CHCl₃, cm⁻¹) 1617, 3019; ¹H NMR (CDCl₃, 200 MHz) δ 8.45 (s, 1H), 7.86-7.93 (m, 2H), 7.16-7.27 (m, 4H), 6.92-6.97 (m, 2H), 3.85 (s, 3H); ¹³C NMR (CDCl₃, 50 MHz) δ 165.6, 158.2, 156.6, 144.5, 132.7, 130.3, 122.1, 115.8, 114.3, 55.3; ESI-MS (m/z): 230.08[M+H]⁺.

(E)-1-(4-fluorophenyl)-N-phenylmethanimine (6l)

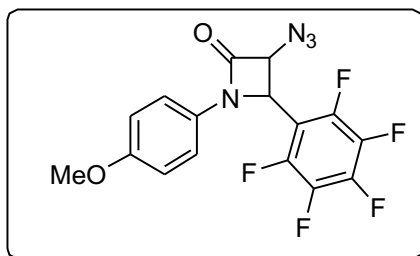


Yield: 80%; M.P 37-38 °C; IR (CHCl₃, cm⁻¹) 1617, 3019; ¹H NMR (CDCl₃, 200 MHz) δ 8.47 (s, 1H), 7.92-7.99 (m, 2H), 7.41-7.49 (m, 2H), 7.17-7.32 (m, 5H); ¹³C NMR (CDCl₃, 50 MHz) δ 167.1, 162.1, 158.7, 151.7, 135.5, 130.8, 129.1, 125.9, 120.8, 116.0, 115.0; ESI-MS (m/z): 200.08[M+H]⁺.

General procedure for synthesis of β-lactams (7+8 a-l)

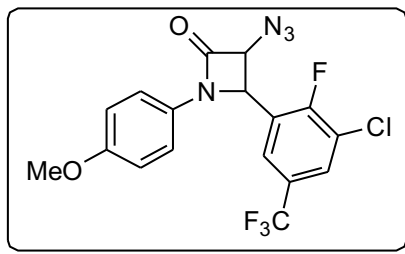
A solution of triphosgene (0.296 g, 1 mmol), in anhydrous CH₂Cl₂ (15 ml), was added slowly to a mixture of potassium salt of azidoacetic acid **3** (2 mmol), imine **6a-l** (2 mmol) and triethyl amine (0.84 ml, 6 mmol) in anhydrous CH₂Cl₂ (20 mL) at 0 °C. After the addition, the reaction mixture was allowed to warm up to room temperature (28 °C) and stirred for 15 h. The reaction mixture was then washed with water (20 ml), saturated sodium bicarbonate solution (2×15 ml) and brine (15 ml). The organic layer was dried over anhydrous sodium sulphate and concentrated to get crude product, which was purified by column chromatography to give pure β-lactams.

3-azido-1-(4-methoxyphenyl)-4-(perfluorophenyl)azetidin-2-one (7+8a)



Yield: 81%; IR (CHCl₃, cm⁻¹) 2115 (N₃), 1763 (CO); ¹H NMR (CDCl₃, 200 MHz) δ 7.20 (d, *J* = 9.09 Hz, 2H), 6.85 (d, *J* = 9.10 Hz, 2H), 5.61 (d, *J* = 5.43, 1H), 5.24 (d, *J* = 5.3, 1H), 3.78 (s, 3H, OCH₃); ¹³C NMR (CDCl₃, 50 MHz) δ 159.7, 157.0, 129.5, 118.1, 114.7, 66.6, 55.4, 51.7; ESI-MS (m/z): 349.06[M+H]⁺.

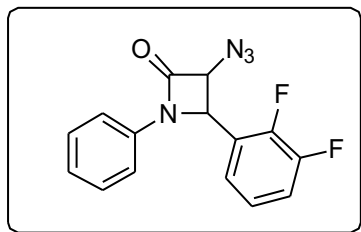
3-azido-4-(3-chloro-2-fluoro-5-(trifluoromethyl)phenyl)-1-(4-methoxyphenyl)azetidin-2-one (7+8b)



Yield: 80%; IR (CHCl₃, cm⁻¹) 2115 (N₃), 1751 (CO); ¹H NMR (CDCl₃, 200 MHz) δ 7.72-7.76 (m, 1H), 7.33-7.36 (m, 1H), 7.22-7.26 (m, 2H), 6.84-6.89 (m, 2H), 5.58 (d, *J* = 5.43, 1H), 5.20 (d, *J* = 5.43, 1H), 3.79 (s, 3H, OCH₃); ¹³C NMR (CDCl₃, 50 MHz) δ 160.2, 157.0, 129.4, 128.6,

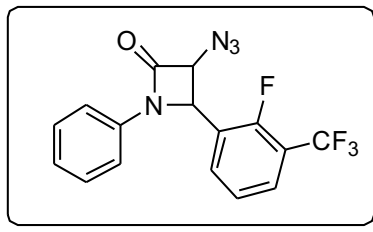
124.1, 118.4, 114.7, 67.2, 55.4, 54.6; ESI-MS (m/z): 415.06[M+H]⁺.

3-azido-4-(2,3-difluorophenyl)-1-phenylazetidin-2-one (7+8c)



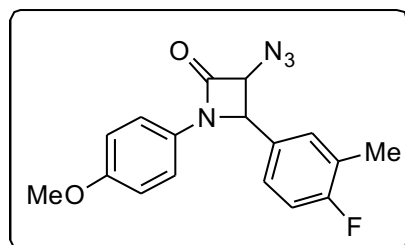
Yield: 77%; IR (CHCl₃, cm⁻¹) 2115 (N₃), 1751 (CO); ¹H NMR (CDCl₃, 200 MHz) δ 7.12-7.25 (m, 5H), 6.91-7.10 (m, 3H), 5.56 (d, *J* = 5.44, 1H), 5.09 (d, *J* = 5.55, 1H); ¹³C NMR (CDCl₃, 50 MHz) δ 161.0, 136.3, 129.3, 129.2, 125.1, 117.3, 117.2, 67.1, 60.1, 54.6; ESI-MS (m/z): 301.06[M+H]⁺.

3-azido-4-(2-fluoro-3-(trifluoromethyl)phenyl)-1-phenylazetidin-2-one (7+8d)



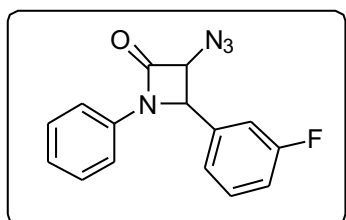
Yield: 75%; IR (CHCl₃, cm⁻¹) 2115 (N₃), 1751 (CO); ¹H NMR (CDCl₃, 200 MHz) δ 7.63-7.70 (m, 1H), 7.36-7.42 (m, 1H), 7.31-7.35 (m, 3H), 7.27-7.30 (m, 1H), 7.14-7.26 (m, 2H), 5.69 (d, *J* = 5.43, 1H), 5.15 (d, *J* = 5.43 Hz, 1H); ¹³C NMR (CDCl₃, 50 MHz) δ 160.9, 136.2, 132.2, 129.4, 125.2, 124.4, 124.3, 117.1, 67.2, 54.2; ESI-MS (m/z): 351.08[M+H]⁺.

3-azido-4-(4-fluoro-3-methylphenyl)-1-(4-methoxyphenyl)azetidin-2-one (7+8e)



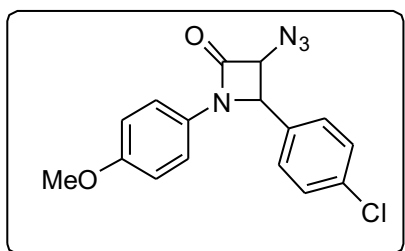
Yield: 52%; IR (CHCl_3 , cm^{-1}) 2115 (N_3), 1751 (CO); ^1H NMR (CDCl_3 , 200 MHz) δ 7.26-7.30 (m, 2H), 7.07-7.20 (m, 3H), 6.83-6.87 (m, 2H), 5.26 (d, $J = 5.31$ Hz, 1H), 5.04 (d, $J = 5.18$ Hz, 1H), 3.80 (s, 3H), 2.31 (s, 3H); ^{13}C NMR (CDCl_3 , 50 MHz) δ 164.0, 160.9, 159.1, 156.6, 130.6, 130.5, 130.0, 127.9, 126.6, 126.4, 118.7, 115.7, 114.4, 67.3, 60.2, 55.4, 49.9, 14.6; ESI-MS (m/z): 326.08[M+H] $^+$.

3-azido-4-(3-fluorophenyl)-1-phenylazetidin-2-one (7+8f)



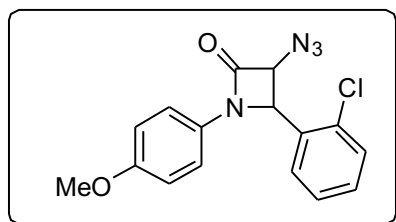
Yield: 81%; IR (CHCl_3 , cm^{-1}) 2115 (N_3), 1751 (CO); ^1H NMR (CDCl_3 , 200 MHz) δ 7.37-7.43 (m, 1H), 7.28-7.32 (m, 4H), 7.12-7.16 (m, 1H), 7.03-7.11 (m, 3H), 5.32 (d, $J = 5.43$, 1H), 5.07 (d, $J = 5.44$ Hz, 1H); ^{13}C NMR (CDCl_3 , 50 MHz) δ 165.4, 161.1, 160.5, 136.4, 135.3, 130.7, 129.3, 125.0, 123.1, 117.3, 114.4, 67.3, 60.1; ESI-MS (m/z): 283.08[M+H] $^+$.

3-azido-4-(4-chlorophenyl)-1-(4-methoxyphenyl)azetidin-2-one (7+8g)



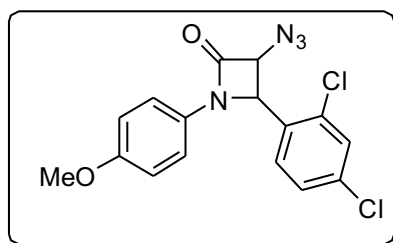
Yield: 90%; IR (CHCl_3 , cm^{-1}) 2115 (N_3), 1751 (CO); ^1H NMR (CDCl_3 , 400 MHz) δ 7.41 (d, $J = 7.82$ Hz, 1H), 7.23-7.29 (m, 4H), 6.83 (d, $J = 8.81$ Hz, 1H), 5.27 (d, $J = 5.38$ Hz, 1H), 5.05 (d, $J = 5.38$ Hz, 1H), 3.77 (s, 3H); ^{13}C NMR (CDCl_3 , 50 MHz) δ 160.6, 156.7, 135.1, 131.2, 129.2, 128.9, 118.7, 114.4, 67.3, 60.1, 55.4; ESI-MS (m/z): 329.08[M+H] $^+$.

3-azido-4-(2-chlorophenyl)-1-(4-methoxyphenyl)azetidin-2-one (7+8h)



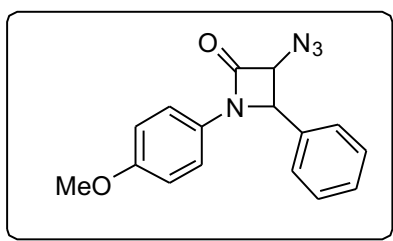
Yield: 91%; IR (CHCl_3 , cm^{-1}) 2115 (N_3), 1751 (CO); ^1H NMR (CDCl_3 , 200 MHz) δ 7.48-7.53 (m, 1H), 7.28-7.36 (m, 2H), 7.21-7.26 (m, 3H), 6.84-6.88 (m, 2H), 5.67 (d, $J = 5.31$, 1H), 5.15 (d, $J = 5.31$ Hz, 1H), 3.79 (s, 3H); ESI-MS (m/z): 329.08[M+H] $^+$.

3-azido-4-(2,4-dichlorophenyl)-1-(4-methoxyphenyl)azetidin-2-one (7+8i)



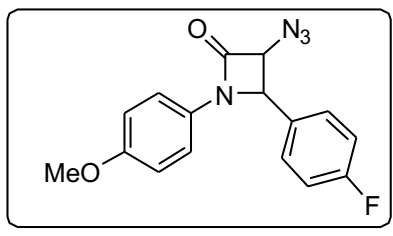
Yield: 90%; IR (CHCl₃, cm⁻¹) 2115 (N₃), 1751 (CO); ¹H NMR (CDCl₃, 200 MHz) δ 7.51 (d, *J* = 1.89 Hz, 1H), 7.20-7.26 (m, 3H), 7.08-7.13 (m, 1H), 6.82-6.87 (m, 2H), 5.59 (d, *J* = 5.31, 1H), 5.15 (d, *J* = 5.30 Hz, 1H), 3.78 (s, 3H); ¹³C NMR (CDCl₃, 50 MHz) δ 160.4, 156.8, 135.3, 129.7, 127.5, 118.5, 114.5, 67.5, 57.9, 55.4; ESI-MS (m/z): 363.04[M+H]⁺.

3-azido-1-(4-methoxyphenyl)-4-phenylazetidin-2-one (7+8j)



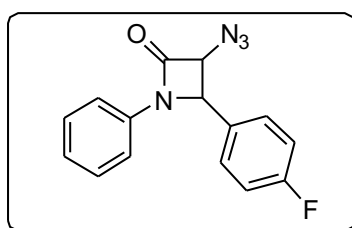
Yield: 94%; IR (CHCl₃, cm⁻¹) 2115 (N₃), 1751 (CO); ¹H NMR (CDCl₃, 200 MHz) δ 7.25-7.41 (m, 6H), 6.68-6.84 (m, 3H), 5.30 (d, *J* = 5.30, 1H), 5.03 (d, *J* = 5.31 Hz, 1H), 3.76 (s, 3H); ¹³C NMR (CDCl₃, 50 MHz) δ 160.8, 156.5, 132.6, 129.1, 128.8, 127.5, 118.7, 114.4, 67.3, 60.7, 55.4; ESI-MS (m/z): 295.14[M+H]⁺.

3-azido-4-(4-fluorophenyl)-1-(4-methoxyphenyl)azetidin-2-one (7+8k)



Yield: 92%; IR (CHCl₃, cm⁻¹) 2115 (N₃), 1751 (CO); ¹H NMR (CDCl₃, 200 MHz) δ 7.29-7.36 (m, 2H), 7.07-7.22 (m, 3H), 6.68-6.84 (m, 3H), 5.28 (d, *J* = 5.31, 1H), 5.03 (d, *J* = 5.31 Hz, 1H), 3.77 (s, 3H); ¹³C NMR (CDCl₃, 50 MHz) δ 164.3, 161.8, 160.6, 156.6, 129.9, 129.4, 128.4, 118.7, 114.4, 67.3, 60.1, 55.4; ESI-MS (m/z): 313.14[M+H]⁺.

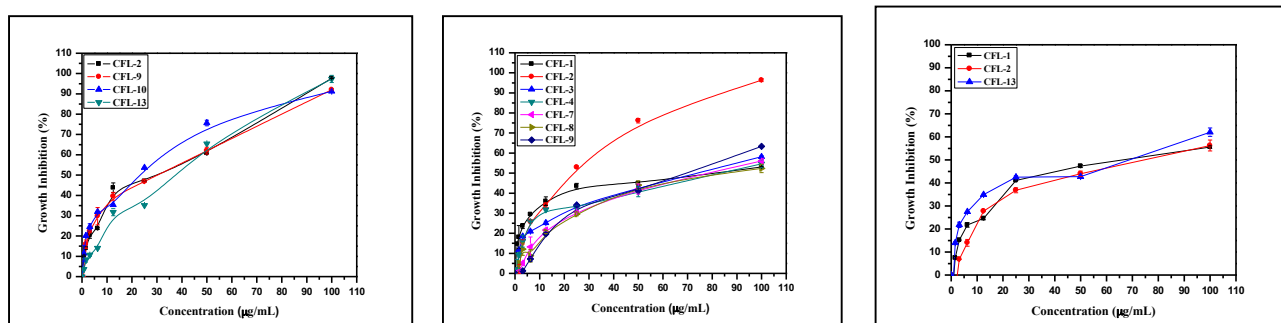
3-azido-4-(4-fluorophenyl)-1-phenylazetidin-2-one (7+8l)



Yield: 72%; IR (CHCl₃, cm⁻¹) 2115 (N₃), 1751 (CO); ¹H NMR (CDCl₃, 200 MHz) δ 7.28-7.51 (m, 5H), 7.05-7.25 (m, 4H), 5.30 (d, *J* = 5.43, 1H), 5.03 (d, *J* = 5.30 Hz, 1H); ¹³C NMR (CDCl₃, 50 MHz) δ 165.4, 161.1, 160.5, 136.4, 135.3, 130.7, 129.3, 125.0, 123.1, 117.3, 114.4, 67.3, 60.1; ESI-MS (m/z): 283.10[M+H]⁺.

Table 1S. Cytotoxicity testing of the compounds 12 (a-l)

Sr. No.	Code	Cytotoxic Effect of inhibitors: MCF-7		Cytotoxic Effect of inhibitors: A431		Cytotoxic Effect of inhibitors: HUVEC	
		IC50	MIC	IC50	MIC	IC50	MIC
1	12a	>100	>100	80.43	>100	63.17	>100
2	12b	31.71	89.67	23.21	83.56	73.83	>100
3	12c	>100	>100	73.74	>100	>100	>100
4	12d	>100	>100	85.76	>100	>100	>100
5	12e	>100	>100	>100	>100	>100	>100
6	12f	>100	>100	>100	>100	>100	>100
7	12g	>100	>100	77.99	>100	>100	>100
8	12h	>100	>100	86.25	>100	>100	>100
9	12i	29.85	97.44	67.77	>100	>100	>100
10	12j	>100	>100	>100	>100	>100	>100
11	12k	>100	>100	>100	>100	>100	>100
12	12l	37.09	88.2	>100	>100	74.14	>100



Experimental: Molecular Docking

Molecular docking study was carried out using the Glide (Grid-Based Ligand Docking with Energetics) module incorporated in the Schrödinger molecular modeling package (Schrödinger, LLC, New York, NY, 2016) Friesner, R.A et. al,¹Halgren, T. A. et.al,²Friesner, R. A. et. al.³to gauge the binding affinity of the new fluconazole β-lactam conjugates linked via 1,2,3-triazole towards sterol 14α-demethylase (CYP51) enzyme in an effort to augment the understanding of their action as antifungal agents. With this purpose, the X-ray crystal structure of sterol 14α-demethylase (CYP51) in complex with Fluconazole was retrieved from the Protein Data Bank

(PDB) (www.rcsb.org) (PDB code: 3KHM). The enzyme-inhibitor complex was preprocessed for docking simulation using the *Protein Preparation Wizard* integrated in the docking program which involved eliminating all the crystallographically observed water molecules (as no water molecule was found to be conserved in the interaction with the enzyme), addition of missing hydrogens/side chain atoms, assigning the correct bond orders and the appropriate charge and protonation state to the protein structure. The missing hydrogens/side chain atoms were corresponding to pH 7.0 considering the appropriate ionization states for the acidic as well as basic amino acid residues. Finally the prepared complex was subjected to energy minimization using the Optimized Potentials for Liquid Simulations-2005 (OPLS-2005) force field, in order to relieve the steric clashes among the residues caused due to addition of hydrogen atoms, until the average root mean square deviation (r.m.s.d.) reached 0.3Å. The 3D structures of title compounds were sketched with the *build* panel in Maestro and optimized with the *ligprep* module which performs addition of hydrogens, adjusting realistic bond lengths and angles, correct the chiralities, ionization states and ring conformations and generation of tautomers,. Partial charges were assigned OPLS-2005 force-field and the resulting structures were further optimized by energy minimization until a energy gradient of 0.001 kcal/mol/Å is reached. After ensuring that the enzyme and ligands were in the correct form, the active site of the enzyme was defined for docking calculation using the *Receptor Grid Generation* panel in Glide which generates two cubical boxes having a common centroid to organize the calculations: a larger enclosing and a smaller binding box. With the non-covalently bound native ligand-fluconazole in place, the active site (receptor) grid was defined by a box that has dimensions of 10X10X10Å centered on the centroid of fluconazole in the crystal complex which was large enough to explore a large portion of the enzyme. The optimized enzyme and ligand structures were then used as input for the docking simulation utilizing the *extra precision* (XP) Glide scoring function to rank the docking poses and to estimate the binding affinities of the ligands to the CYP51 target. The *extra precision* (XP) scoring function in Glide is equipped with force field-based parameters accounting for contributions from steric interactions and electrostatic energies as well as solvation and repulsive interactions along with hydrophobic, hydrogen bonding and metal-ligand interactions all integrated in the empirical energy functions. The output files in terms of the docking poses of the ligands were visualized and analyzed key elements of interaction with the enzyme using the Maestro's Pose Viewer utility. Meanwhile, to validate the accuracy of the

docking protocol the co-crystallized ligand (fluconazole) was extracted from the crystal structure and re-docked into the active site defining the above mentioned parameters (**Figure 1S**). A very good agreement was observed between the localization of the fluconazole upon docking and from the X-ray bound conformation with an rmsd of less than 1.0Å indicating the reliability of the docking protocol in accurately predicting the binding mode for the title molecules.

Table 2S: Quantitative estimates of the per-residue interaction analysis of the fluconazole β -lactam conjugates (**12a-I**) with sterol 14 α -demethylase (CYP51).

Compound ID	MIC	Docking score	Binding energy	Per-residue interaction energy analysis		
				van der Waals (kcal/mol)	Electrostatic (kcal/mol)	$\pi-\pi$ stacking (Å)
12a	0.50	-7.46	-53.38	Heme500(-5.67), Val461(-1.124), Thr459(-1.31), Leu356(-1.30), His294(-1.22), Phe290(-3.07), Ala287(-1.26), Leu208(-2.65), Glu205(-1.33), Leu127(-1.01), Phe110(-1.29), Met106(-1.60), Ile105(-1.19), Tyr103(-1.95)	Heme500(-3.80), Tyr116(-1.58)	His294(2.04), Tyr116(1.86)
12b	0.25	-7.61	-55.12	Heme500(-6.55), Val461(-2.07), Met460(-2.40), Thr459(-1.43), Thr295(-1.12), His294(-2.06), Ala291(-1.10), Ala287(-1.47), Leu208(-2.00), Glu205(-1.76), Leu127(-1.03), Tyr116(-2.83), Phe110(-1.73), Met106(-1.18), Ile105(-1.94), Tyr103(-2.28)	Heme500(-4.39), Glu205(-1.20), Tyr116(-1.81)	Tyr103(2.40), Tyr116(2.29), His294(2.56)
12c	0.25	-7.58	-55.54	Heme500(-6.80), Met460(-2.17), Thr459(-1.36), Leu356(-1.90), Thr295(-1.13), His294(-2.10), Ala291(-1.15), Phe290(-3.16), Leu208(-2.62), Glu205(-1.75), Tyr116(-2.61), Phe110(-1.39), Ile105(-1.20),	Heme500(-4.11), Phe290(-1.60), Glu205(-1.72), Tyr116(-1.52)	Tyr103(2.35), His294(2.30)

				Tyr103(-2.18)		
12d	0.50	-7.40	-53.12	Heme500(-5.50), Met460(-2.11), Thr459(-1.16), Thr295(-1.09), His294(-2.18), Ala291(-1.14), Phe290(-2.53), Ala287(-1.04), Leu208(-2.13), Glu205(-1.32), Leu127(-1.20), Tyr116(-2.16), Phe110(-1.42), Ile105(-1.08), Tyr103(-1.71)	Heme500(-3.80), Phe290(-1.14), Glu205(-1.17)	Phe110(2.84), Phe290(2.49), His294(2.24)
12e	0.25	-7.54	-55.10	Heme500(-6.33), Val461(-1.93), Met460(-2.37), Thr459(-1.56), Leu356(-1.80), Thr295(-1.26), His294(-2.15), Ala291(-1.19), Phe290(-3.58), Ala287(-1.56), Leu208(-3.11), Glu205(-1.80), Leu127(-1.13), Tyr116(-2.54), Phe110(-1.46), Met106(-1.77), Ile105(-1.24), Tyr103(-2.15)	Heme500(-4.14), Phe290(-1.07), Tyr116(-1.85)	Tyr103(2.40), Tyr116(2.30), His294(2.40)
12f	0.125	-7.95	-56.27	Heme500(-7.38), Met460(-3.18), Thr459(-1.91), Leu356(-2.16), Thr295(-1.13), His294(-2.09), Ala291(-1.12), Phe290(-3.81), Ala287(-1.78), Leu208(-2.96), Glu205(-1.67), Leu127(-1.04), Tyr116(-3.33), Phe110(-1.87), Ile105(-2.16), Tyr103(-2.194)	Heme500(-4.53), Phe290(-1.26), Glu205(-2.51)	Tyr103(2.33), Tyr116(2.28), His294(2.37)
12g	0.125	-7.91	-56.79	Heme500(-7.41), Met460(-3.15), Leu356(-	Heme500(-4.85),	Tyr103(2.2

				2.14), Thr295(-1.16), His294(-2.14), Ala291(-1.32), Phe290(-3.14), Ala287(- 1.74), Leu208(-3.11), Glu205(-1.66), Leu127(-1.03), Tyr116(-3.23), Phe110(- 1.87), Met106(-1.93), Ile105(-1.65), Tyr103(-2.20)	Phe290(-1.13)	7), Tyr116(2.2 7), His294(2.9 1)
12h	0.25	-7.59	-55.99	Heme500(-6.66), Val461(-1.81), Met460(- 2.49), Thr459(-1.63), Leu356(-1.86), Thr295(-1.16), His294(-1.95), Ala291(- 1.62), Phe290(-2.92), Ala287(-1.40), Leu208(-3.12), Glu205(-1.71), Leu127(- 1.16), Tyr116(-2.47), Phe110(-1.49), Ile105(-2.05), Tyr103(-2.35)	Heme500(-4.75), Glu205(-2.38)	Tyr103(2.1 9), Phe110(2.7 8), His294(2.8 1)
12i	0.5	-7.45	-53.95	Heme500(-5.86), Met460(-1.94), Thr459(- 1.01), 422(-1.09), Leu356(-1.33), Thr295(- 1.15), His294(-2.08), Ala291(-1.65), Phe290(-2.10), Leu208(-2.18), Glu205(- 1.15), Phe110(-1.23), Tyr103(-1.75)	Heme500(-3.77), Tyr116(-1.29)	Tyr116(1.8 3)
12j	0.031	-8.50	-58.96	Heme500(-8.82), Val461(-2.59), Met460(- 3.75), Thr459(-2.28), Val359(-1.47), Leu356(-2.74), His294(-2.84), Ala291(- 1.79), Phe290(-4.15), Leu208(-3.48),	Heme500(-5.73), Ala291(-1.36), Phe290(-1.41), Glu205(-2.51),	His294(2.3 1)

				Glu205(-2.54), Tyr116(-4.21), Phe110(-2.13), Met106(-2.03), Ile105(-2.40), Tyr103(-2.95)	Tyr116(-1.94), Tyr103(-1.23)	
12k	0.0625	-8.28	-57.89	Heme500(-8.29), Val461(-2.20), Met460(-3.37), Thr459(-2.18), Leu356(-2.24), Thr295(-1.44), His294(-2.29), Ala291(-1.21), Phe290(-4.03), Ala287(-1.74), Leu208(-3.17), Glu205(-1.76), Leu127(-1.12), Tyr116(-3.85), Phe110(-1.82), Met106(-2.01), Ile105(-2.24), Tyr103(-2.24)	Heme500(-4.96), Ala291(-1.10), Phe290(-1.17), Tyr116(-1.88)	Tyr116(2.24), His294(2.52)
12l	0.25	-7.69	-55.82	Heme500(-6.45), Met460(-2.36), Thr459(-1.62), Leu356(-1.45), Thr295(-1.10), His294(-1.71), Phe290(-4.02), Ala287(-1.77), Leu208(-2.80), Glu205(-1.96), Leu127(-1.13), Tyr116(-2.28), Phe110(-1.55), Met106(-2.04), Ile105(-1.99), Tyr103(-2.18)	Heme500(-4.11), Phe290(-1.17)	Tyr103(2.34), Tyr116(2.27), His294(2.59)

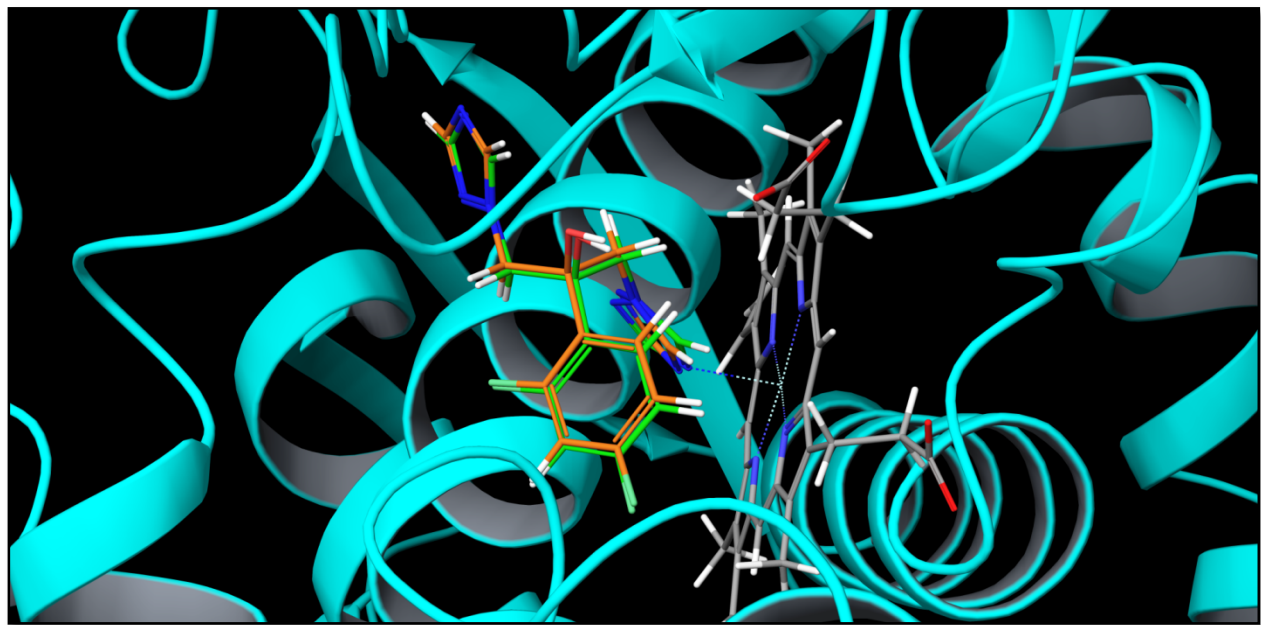


Figure 1S: Validation of docking protocol: Overlay of the best scoring pose for native ligand-Fluconazole obtained by docking (green carbon) against the X-ray bound conformation (orange carbon).

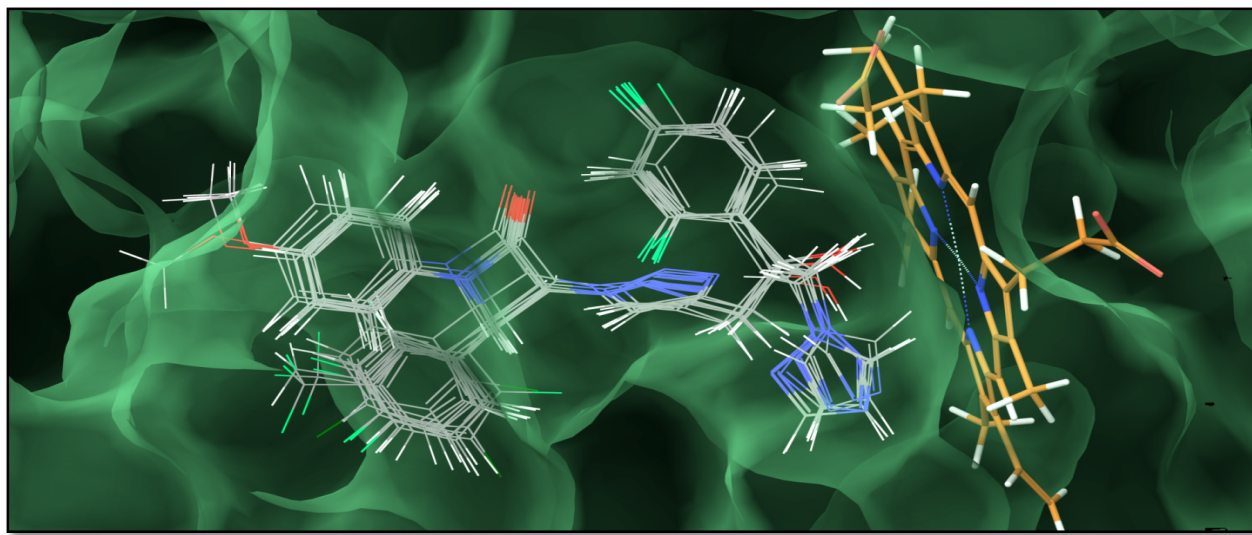


Figure 2S. Binding mode of fluconazole β-lactam conjugates linked via 1,2,3-triazole **12 (a-l)** into the active site of fungal sterol 14 α -demethylase (CYP51).

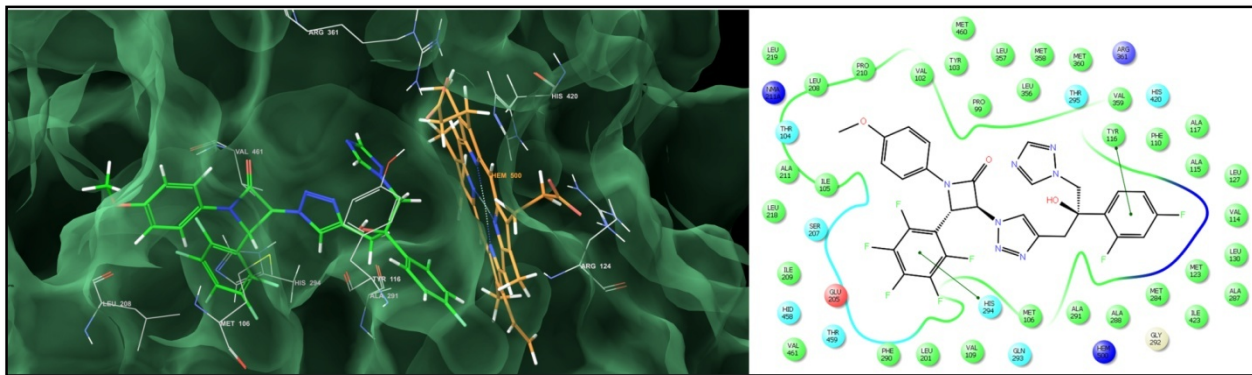


Figure 3S. Binding mode of **12a** into the active site of sterol 14 α -demethylase (CYP51) (the π - π stacking interaction has been represented using green lines).

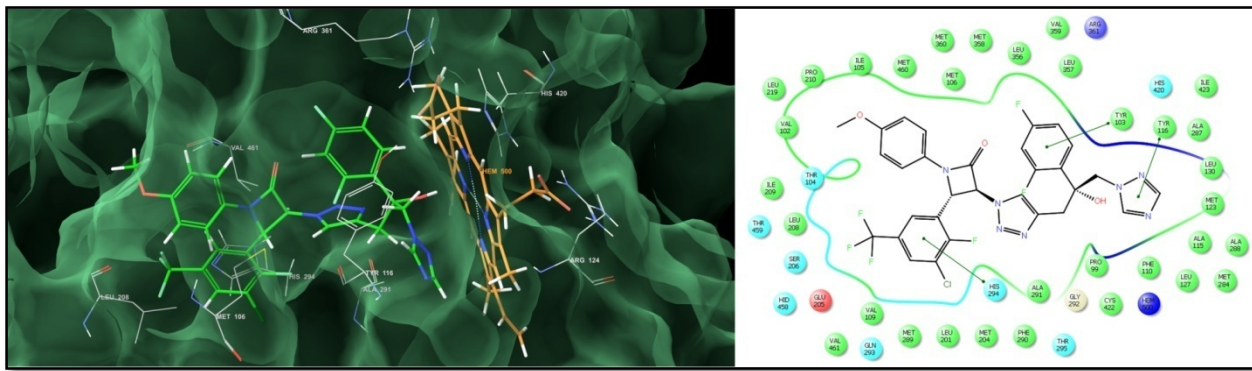


Figure 4S. Binding mode of **12b** into the active site of sterol 14 α -demethylase (CYP51) (the π - π stacking interaction has been represented using green lines).

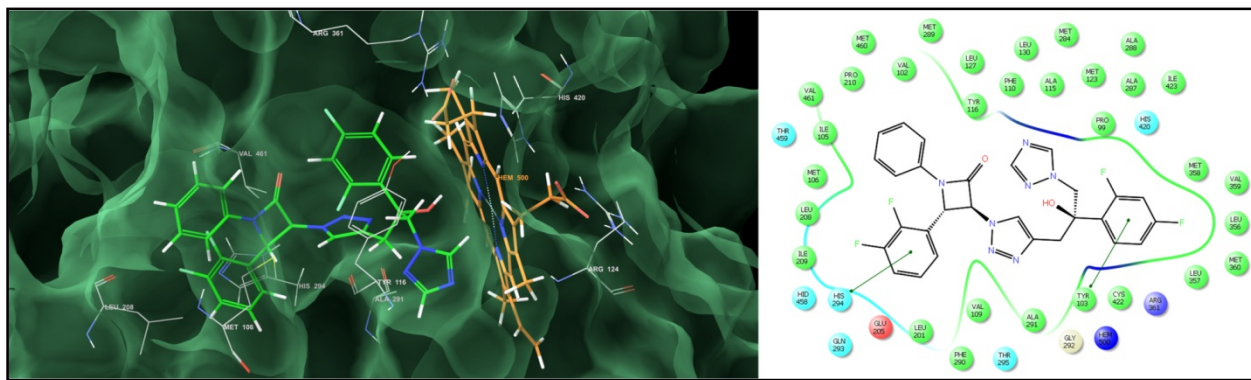


Figure 5S. Binding mode of **12c** into the active site of sterol 14 α -demethylase (CYP51) (the π - π stacking interaction has been represented using green lines).

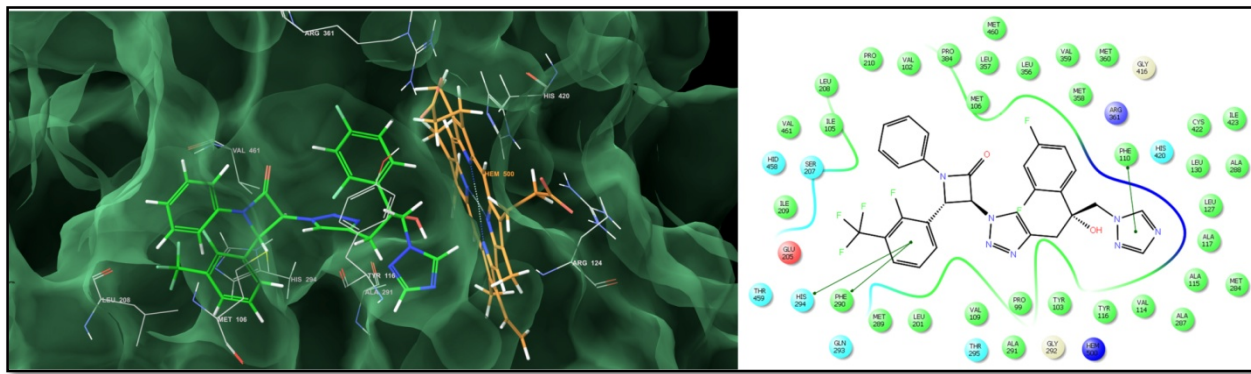


Figure 6S. Binding mode of **12d** into the active site of sterol 14 α -demethylase (CYP51) (the π - π stacking interaction has been represented using green lines).

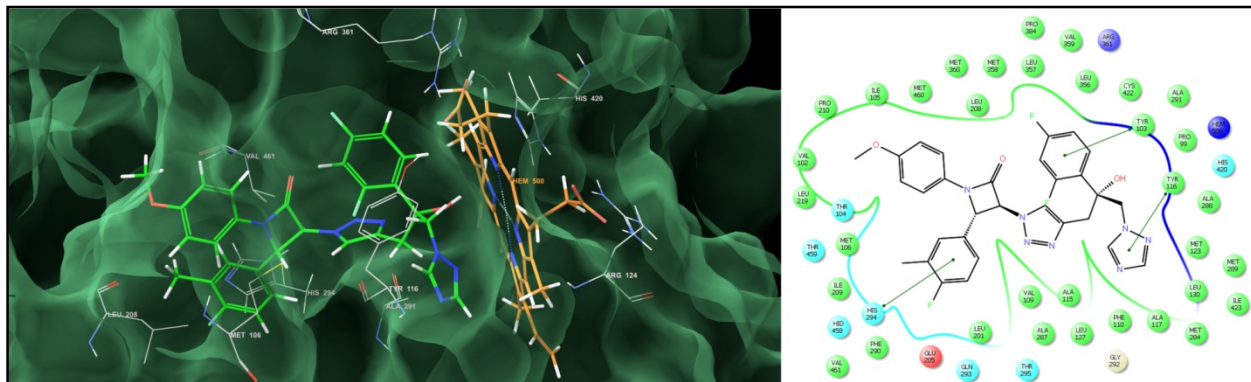


Figure 7S. Binding mode of **12e** into the active site of sterol 14 α -demethylase (CYP51) (the π - π stacking interaction has been represented using green lines).

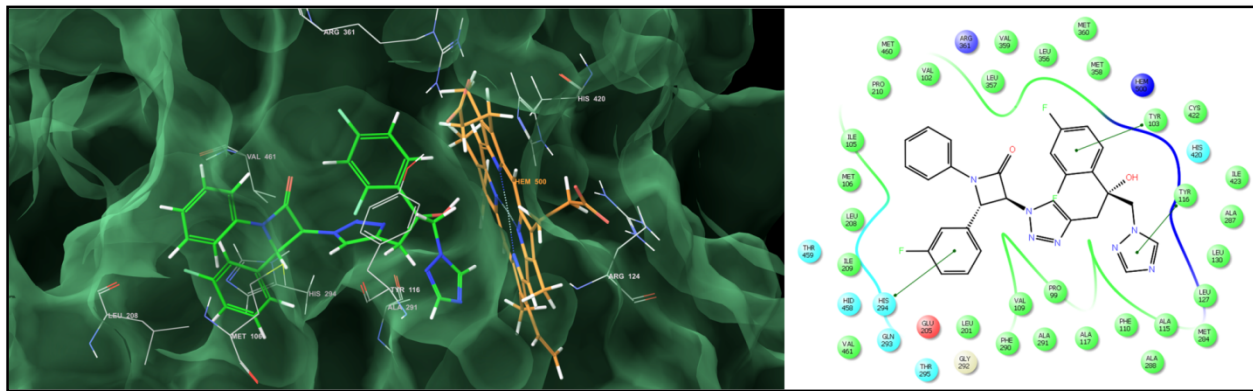


Figure 8S. Binding mode of **12f** into the active site of sterol 14 α -demethylase (CYP51) (the π - π stacking interaction has been represented using green lines).

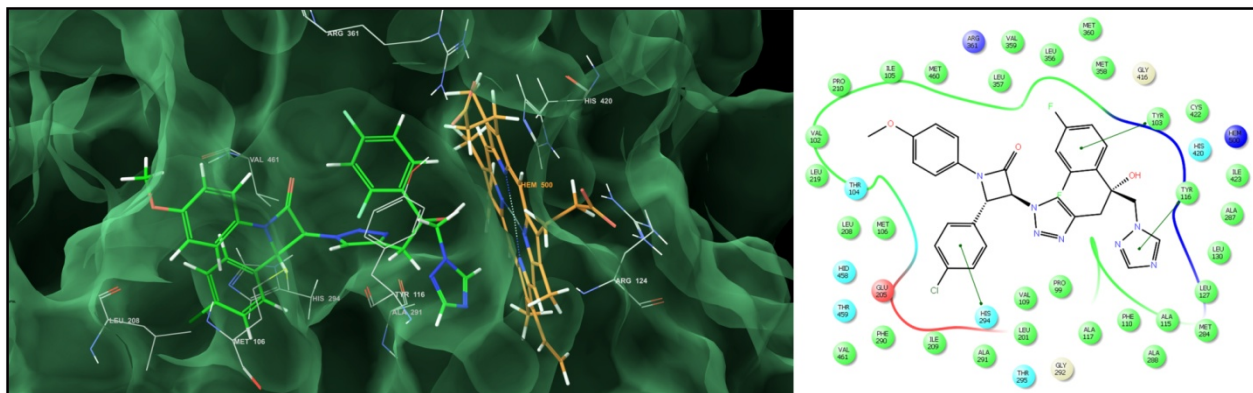


Figure 9S. Binding mode of **12g** into the active site of sterol 14 α -demethylase (CYP51) (the π - π stacking interaction has been represented using green lines).

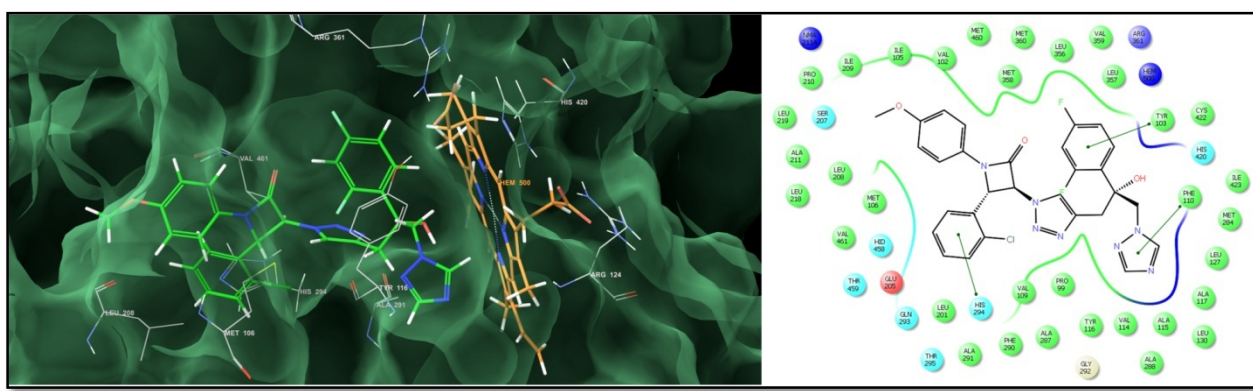


Figure 10S. Binding mode of **12h** into the active site of sterol 14 α -demethylase (CYP51) (the π - π stacking interaction has been represented using green lines).

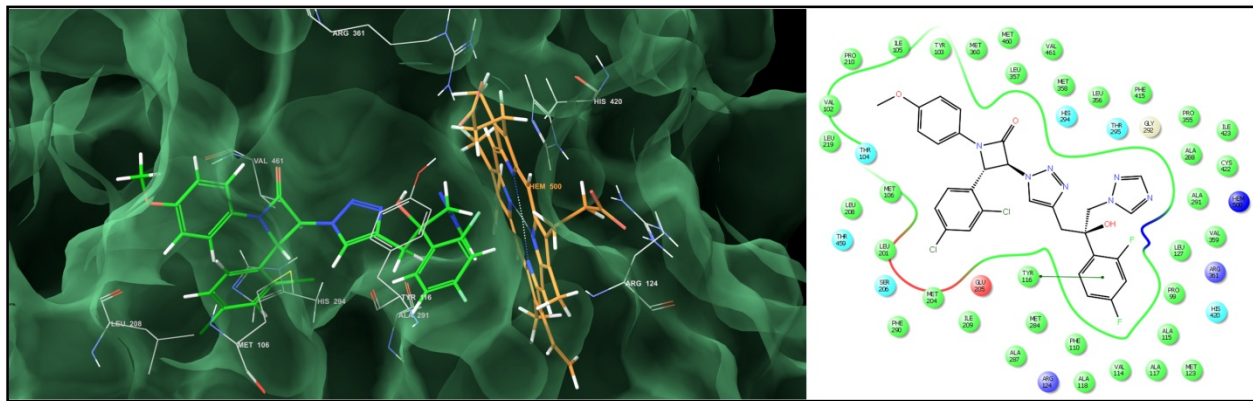


Figure 11S. Binding mode of **12i** into the active site of sterol 14 α -demethylase (CYP51) (the $\pi-\pi$ stacking interaction has been represented using green lines).

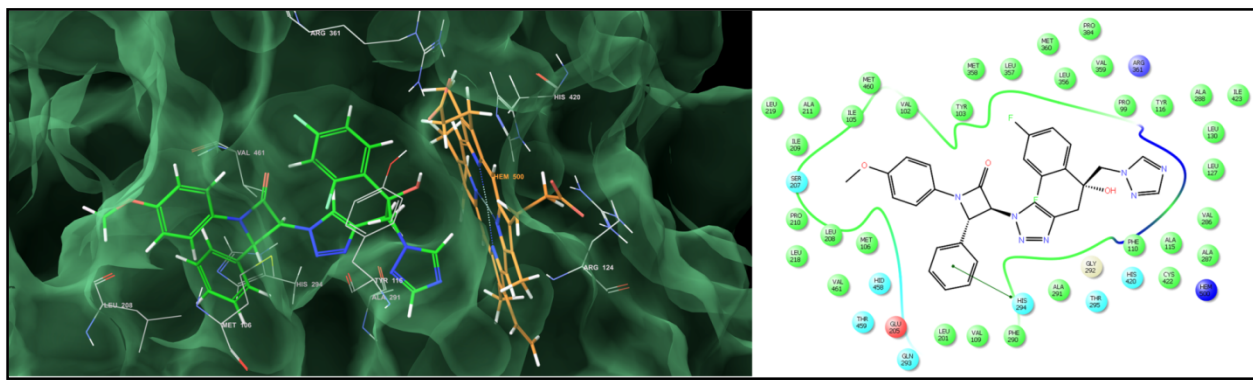


Figure 12S. Binding mode of **12j** into the active site of sterol 14 α -demethylase (CYP51) (the $\pi-\pi$ stacking interaction has been represented using green lines).

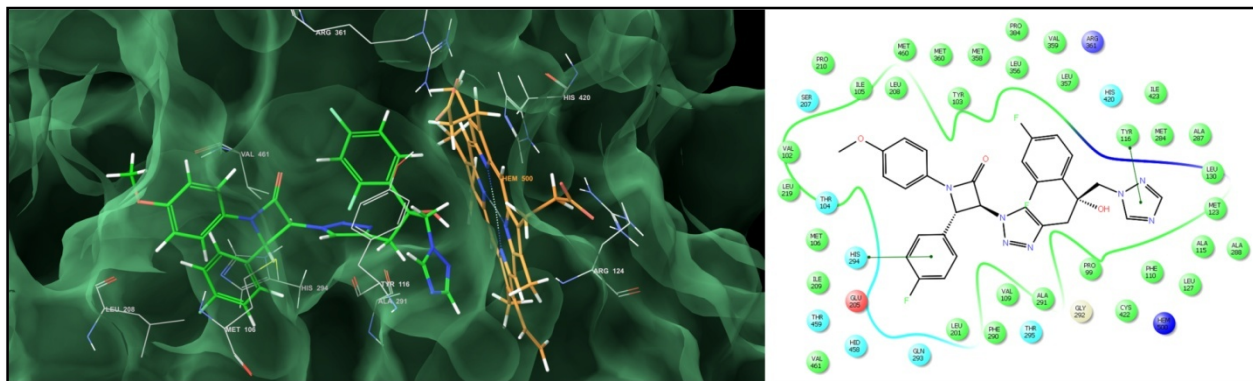


Figure 13S. Binding mode of **12k** into the active site of sterol 14 α -demethylase (CYP51) (the $\pi-\pi$ stacking interaction has been represented using green lines).

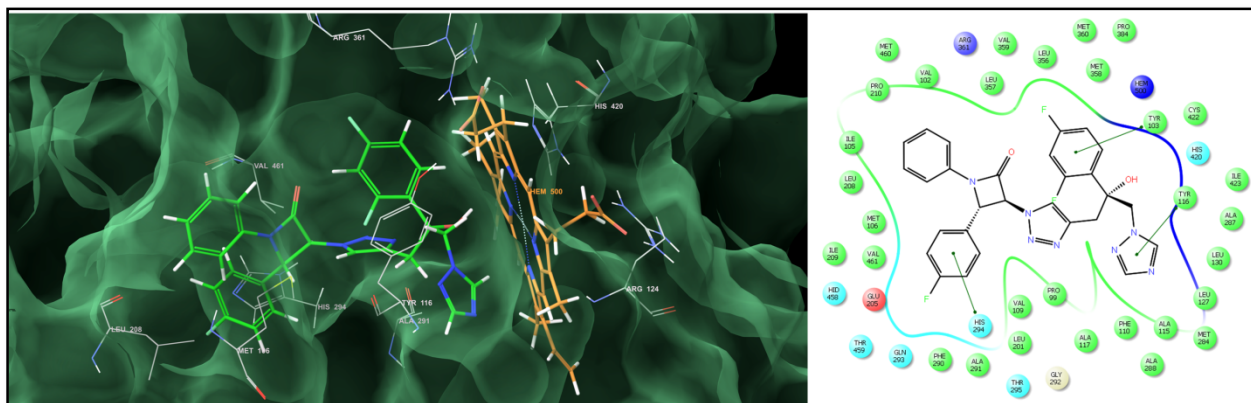


Figure 14S. Binding mode of **12l** into the active site of sterol 14 α -demethylase (CYP51) (the π - π stacking interaction has been represented using green lines).

MTT assay (MTT: MTT (3-(4,5-Dimethylthiazol-2-yl)-2,5-Diphenyltetrazolium Bromide))

In vitro cytotoxicity against above mentioned human cell lines was determined using MTT assay as described previously (Ciapetti et al, 1983).^{4,5} Briefly, log phase cells were harvested using trypsin (0.05% trypsin, 0.02% EDTA, in PBS) from tissue culture flask and the suspension was diluted with appropriate culture medium to obtain cell density of 10^5 cells/mL as determined by hemocytometry. An aliquot of 100 μ l (10^4 cells/well) of each suspension was seeded in 96-wells cell culture plates and these were incubated at 37°C in an atmosphere of 5% CO₂ and 95% relative humidity in a CO₂ incubator. After 24 h, compounds (1 μ l/well) at varying concentrations of 100 to 0.7825 μ g/ml were added to the wells containing cells. Paclitaxel, Carboplatin, Doxorubicin were used as positive control. Suitable controls with equivalent concentration of DMSO were also included. The plates were further incubated for 48 h., at the end of the incubation period; the solution containing the unattached cells was discarded followed by addition of 10 μ L MTT (5 mg/mL in PBS) to adhered cells in growth medium. After 3.5 h at 37°C for MTT cleavage, the formazan product was solubilized by the addition of 100 μ L 0.04 N HCl in isopropanol. Absorbance was measured on a SPECTRAmax PLUS 384 plate reader at wavelength of 570 nm. Percentage cytotoxicity was calculated using the formula-

$$\% \text{ Cytotoxicity} = [(\text{Control} - \text{CMP}) / (\text{Control} - \text{blank})] \times 100$$

Where, Control = cell growth in medium without compounds

CMP = cell growth in presence of compounds

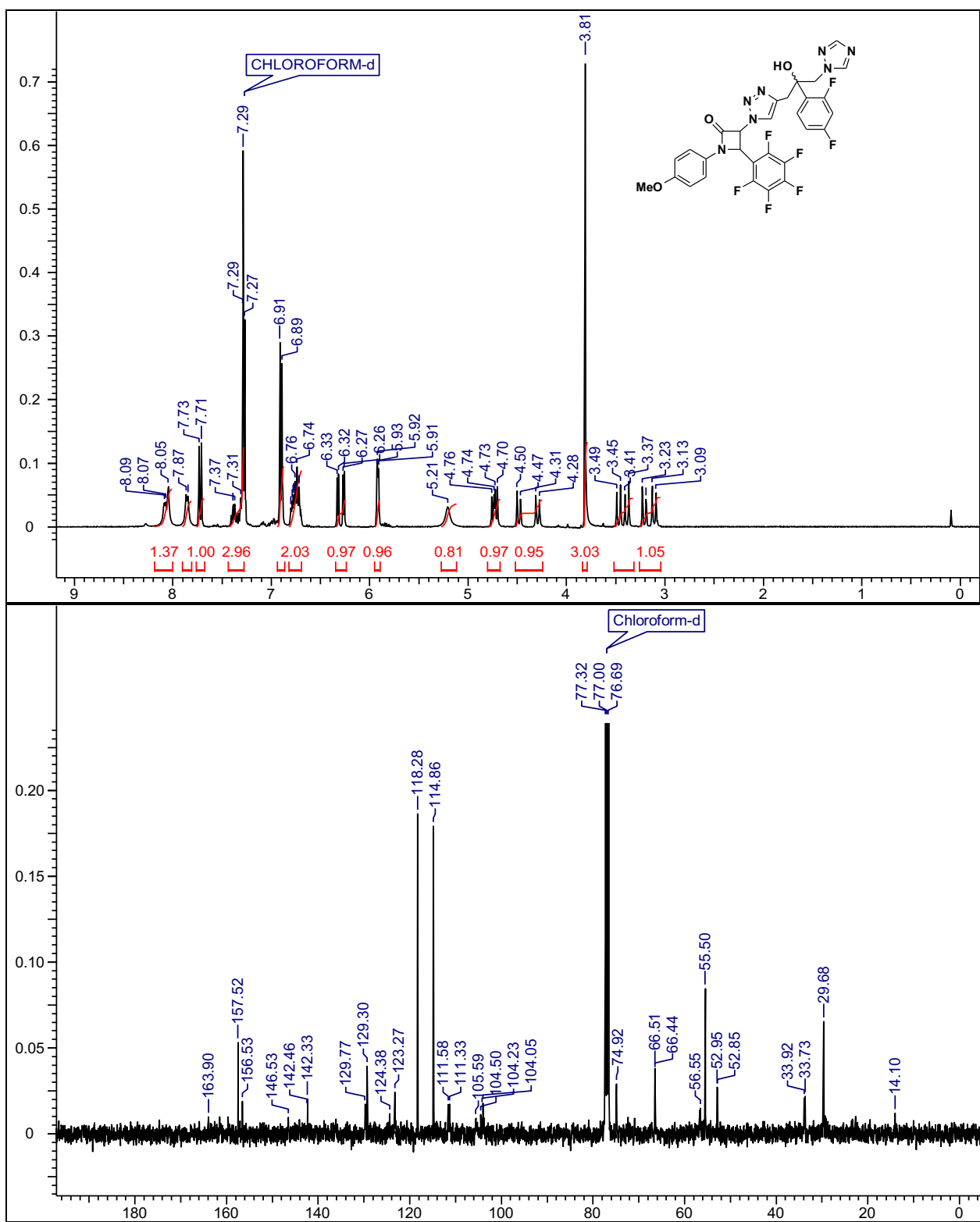
Blank = culture medium without cells

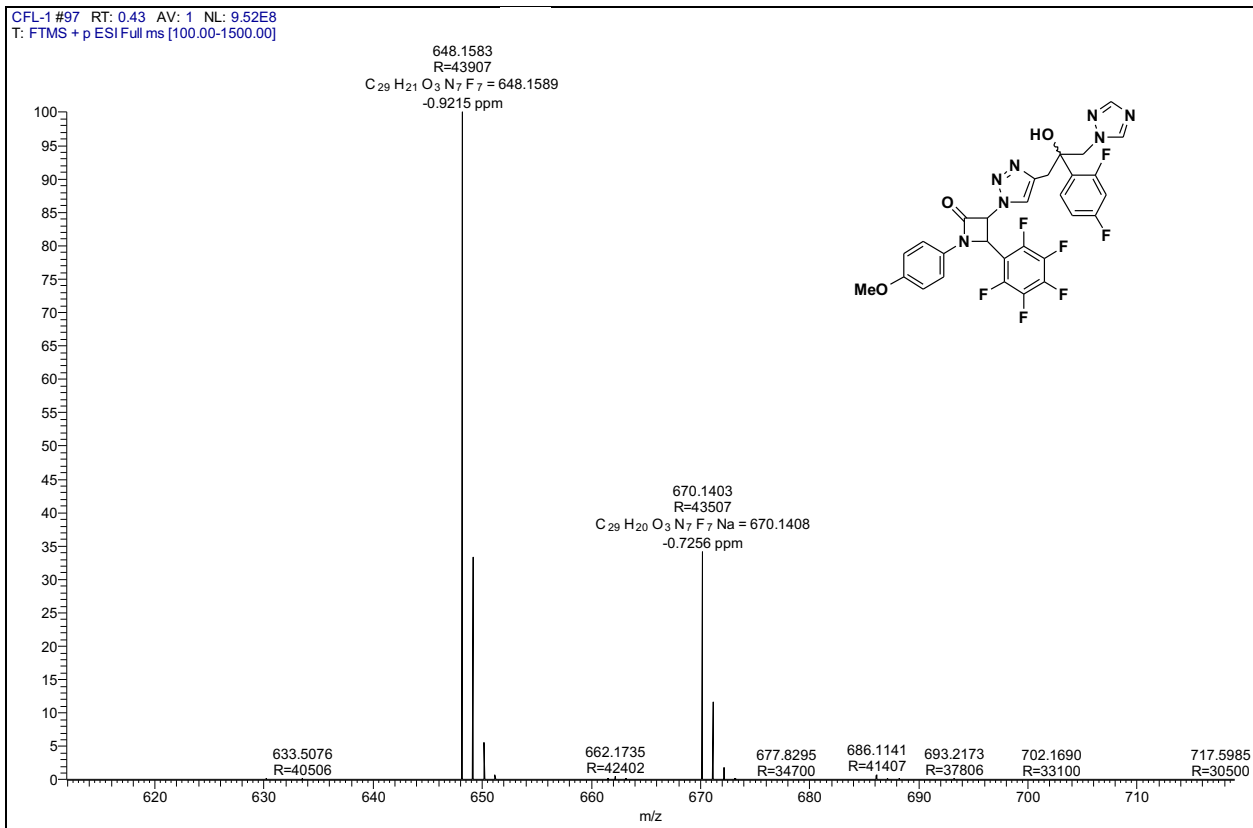
Experiment was performed in triplicates and the quantitative value was expressed as the average ± standard deviation.

Experimental Data

*3-(4-(2-(2,4-difluorophenyl)-2-hydroxy-3-(1*H*-1,2,4-triazol-1-yl)propyl)-1*H*-1,2,3-triazol-1-yl)-1-(4-methoxyphenyl)-4-(perfluorophenyl)azetidin-2-one ; 12a.* Yield: 90%; IR (CHCl³, cm⁻¹) 3415, 1761; ¹H NMR (CDCl₃, 400 MHz) δ 8.05-8.09 (m, 1H), 7.85 (d, *J*= 7.3 Hz, 1H), 7.71 (d, *J*= 9.5Hz, 1H), 7.29 (d, *J*= 8.0 Hz, 2H, Ar-H), 7.31-7.40 (m, 1H, Ar-H), 6.89 (d, *J*= 9.0 Hz, 2H), 6.70-6.80 (m, 2H), 6.26-6.33 (m, 1H), 5.91-5.93 (m, 1H), 5.21 (bs, 1H), 4.70-4.76 (m, 1H), 4.28-4.50 (m, 1H), 3.81 (s, 3H), 3.37-3.49 (m, 1H), 3.09-3.23 (m, 1H); ¹³C NMR (CDCl₃, 50 MHz) δ 163.9, 157.5, 156.5, 146.5, 142.4, 142.3, 129.7, 129.3, 124.4, 123.2, 118.3, 114.8, 111.6, 111.3, 105.6, 104.5, 104.2, 104.0, 74.9, 66.5, 56.5, 55.5, 52.9, 52.8, 33.9, 33.7, 29.7, 14.1; ESI-MS (m/z): 648.15 [M+H]⁺; HRMS (ESI-qTOF): calcd for C₂₉H₂₁F₇N₇O₃ [M+H]⁺, 648.1589; found: 648.1583.

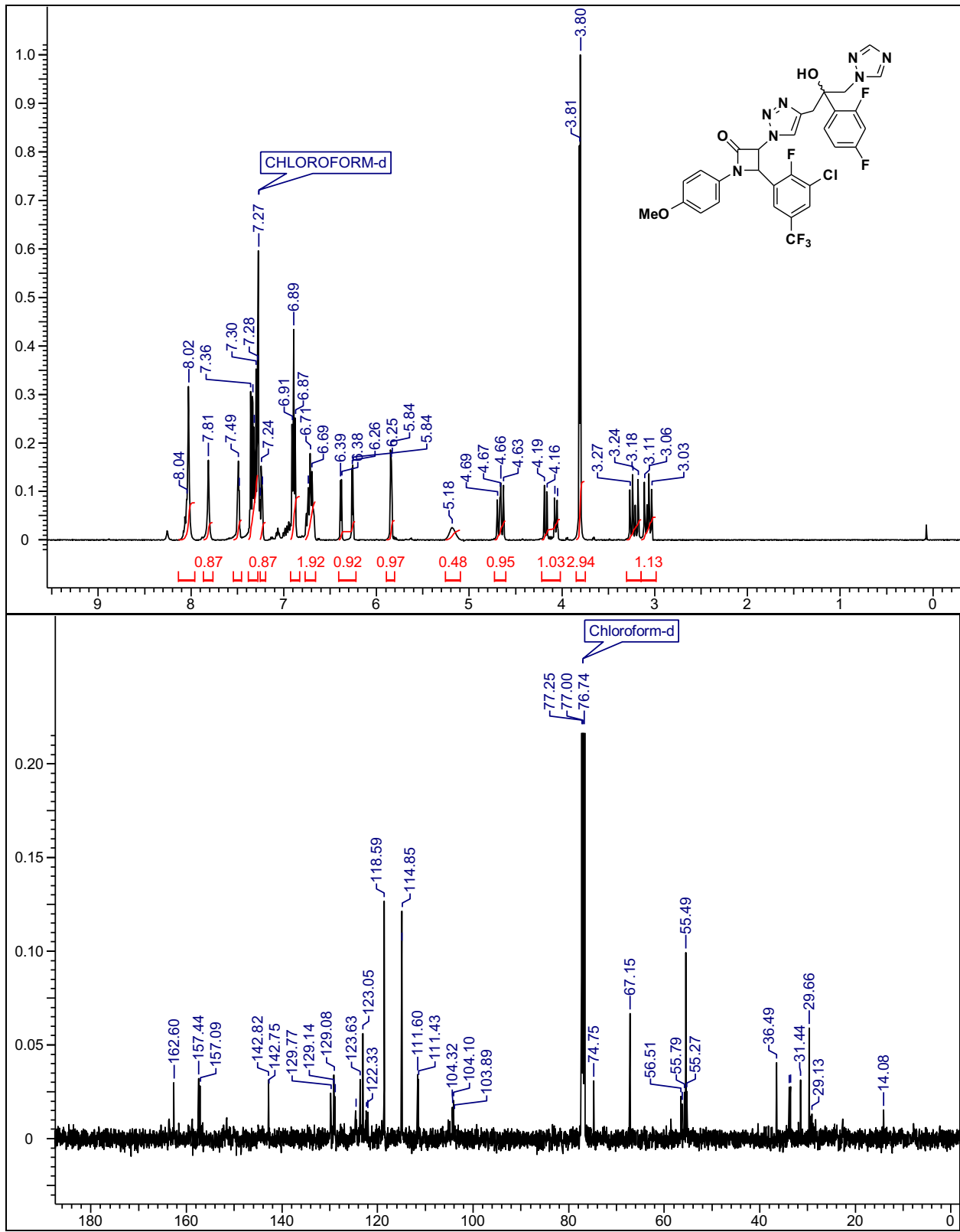
12a

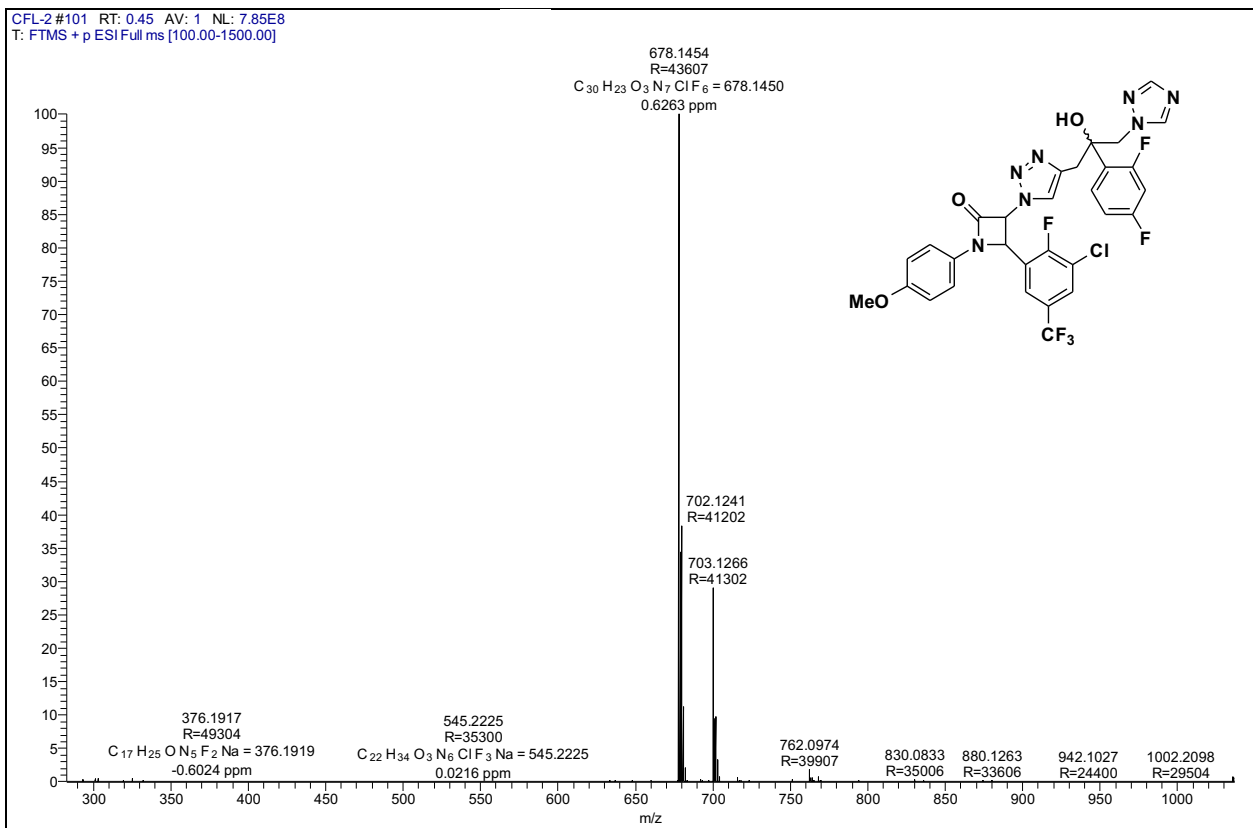




4-(3-chloro-2-fluoro-5-(trifluoromethyl)phenyl)-3-(4-(2-(2,4-difluorophenyl)-2-hydroxy-3-(1*H*-1,2,4-triazol-1-yl)propyl)-1*H*-1,2,3-triazol-1-yl)-1-(4-methoxyphenyl)azetidin-2-one; 12b. Yield: 89%; IR (CHCl_3 , cm^{-1}) 3415, 1761; ^1H NMR (CDCl_3 , 500 MHz) δ 8.02-8.06 (m, 2H), 7.81 (s, 1H), 7.47-7.51 (m, 1H, Ar-H), 7.28-7.36 (m, 3H, Ar-H), 7.23-7.26 (m, 1H, Ar-H), 6.89 (t, J = 8.54 Hz, 2H), 6.67-6.78 (m, 2H), 6.25-6.39 (m, 1H), 5.83-5.84 (m, 1H), 5.18 (bs, 1H), 4.63-4.69 (m, 1H), 4.05-4.19 (m, 1H), 3.81 (s, 3H), 3.18-3.27 (m, 1H), 3.03-3.11 (m, 1H); ^{13}C NMR (CDCl_3 , 50 MHz) δ 162.6, 157.4, 157.1, 142.8, 142.7, 129.8, 129.1, 124.5, 123.6, 123.0, 118.6, 114.8, 111.6, 111.4, 104.3, 104.1, 103.9, 74.7, 67.1, 56.5, 55.8, 55.5, 55.3, 36.5, 33.8, 33.6, 31.4, 29.7, 29.1, 14.1; ESI-MS (m/z): 678.14 [$\text{M}+\text{H}]^+$; HRMS (ESI-qTOF): calcd for $\text{C}_{30}\text{H}_{23}\text{ClF}_6\text{N}_7\text{O}_3$ [$\text{M}+\text{H}]^+$, 678.1450; found: 678.1454.

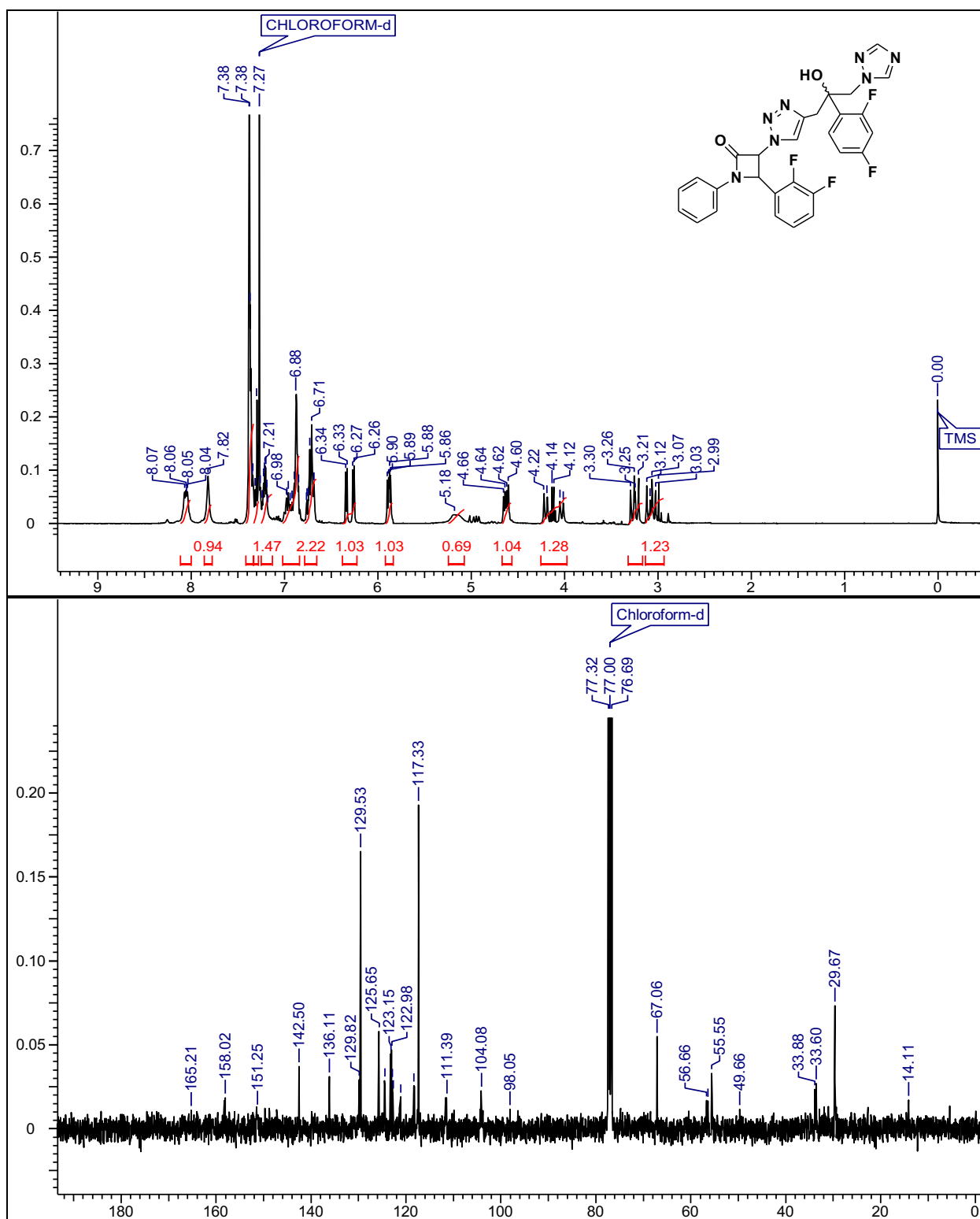
12b

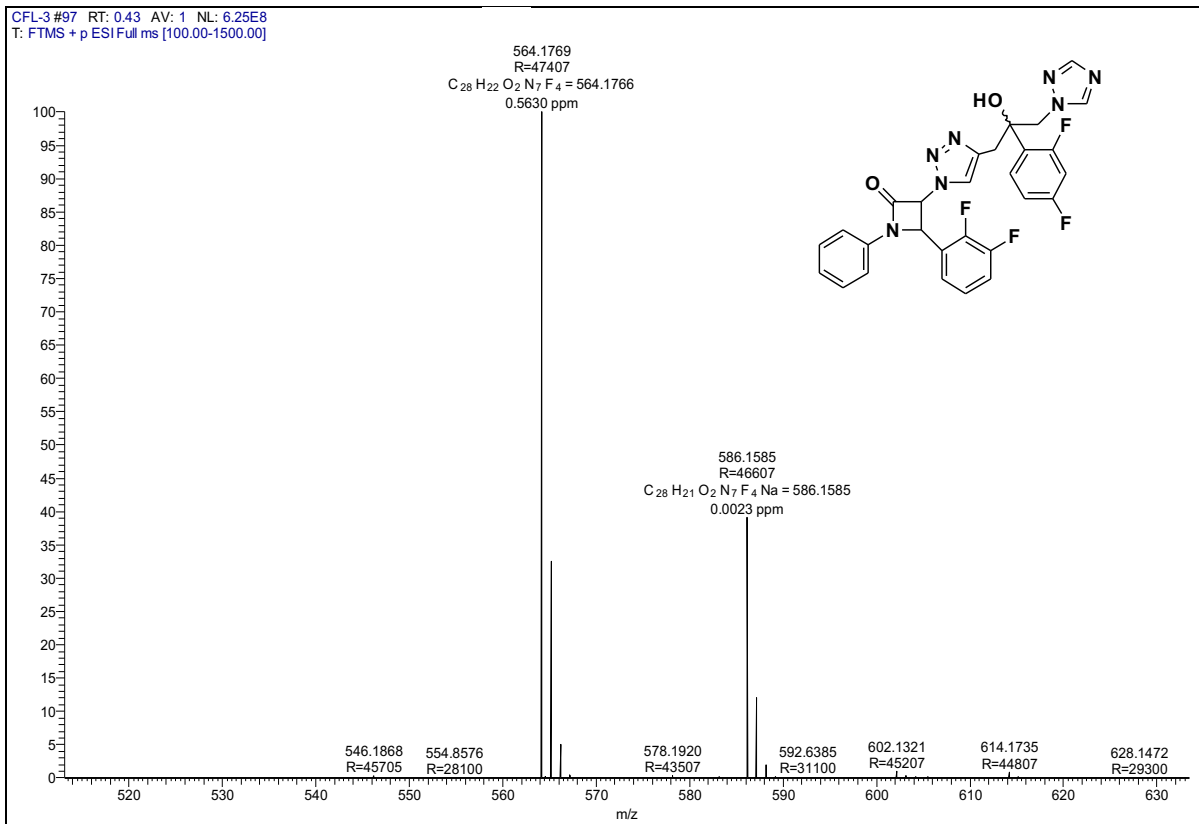




*4-(2,3-difluorophenyl)-3-(4-(2,4-difluorophenyl)-2-hydroxy-3-(1*H*-1,2,4-triazol-1-yl)propyl)-1*H*-1,2,3-triazol-1-yl)-1-phenylazetidin-2-one; 12c.* Yield: 91%; IR (CHCl₃, cm⁻¹) 3415, 1761; ¹H NMR (CDCl₃, 400 MHz) δ 8.03-8.07 (m, 1H), 7.82 (s, 1H), 7.33-7.40 (m, 5H, Ar-H), 7.28-7.31 (m, 1H, Ar-H), 7.18-7.23 (m, 1H, Ar-H), 6.85-6.98 (m, 3H), 6.68-6.76 (m, 2H), 6.25-6.34 (m, 1H), 5.86-5.89 (m, 1H), 5.18 (bs, 1H), 4.60-4.65 (m, 1H), 4.01-4.22 (m, 1H), 3.20-3.29 (m, 1H), 2.99-3.12 (m, 1H); ¹³C NMR (CDCl₃, 50 MHz) δ 165.2, 158.2, 158.0, 151.2, 142.5, 136.1, 129.8, 129.5, 125.6, 123.0, 117.3, 111.4, 104.1, 98.0, 67.0, 56.6, 56.3, 55.5, 49.6, 33.9, 33.6, 29.7, 14.1; ESI-MS(m/z): 564.17[M+H]⁺; HRMS (ESI-qTOF): calcd for C₂₈H₂₂F₄N₇O₂ [M+H]⁺, 564.1766; found: 564.1769.

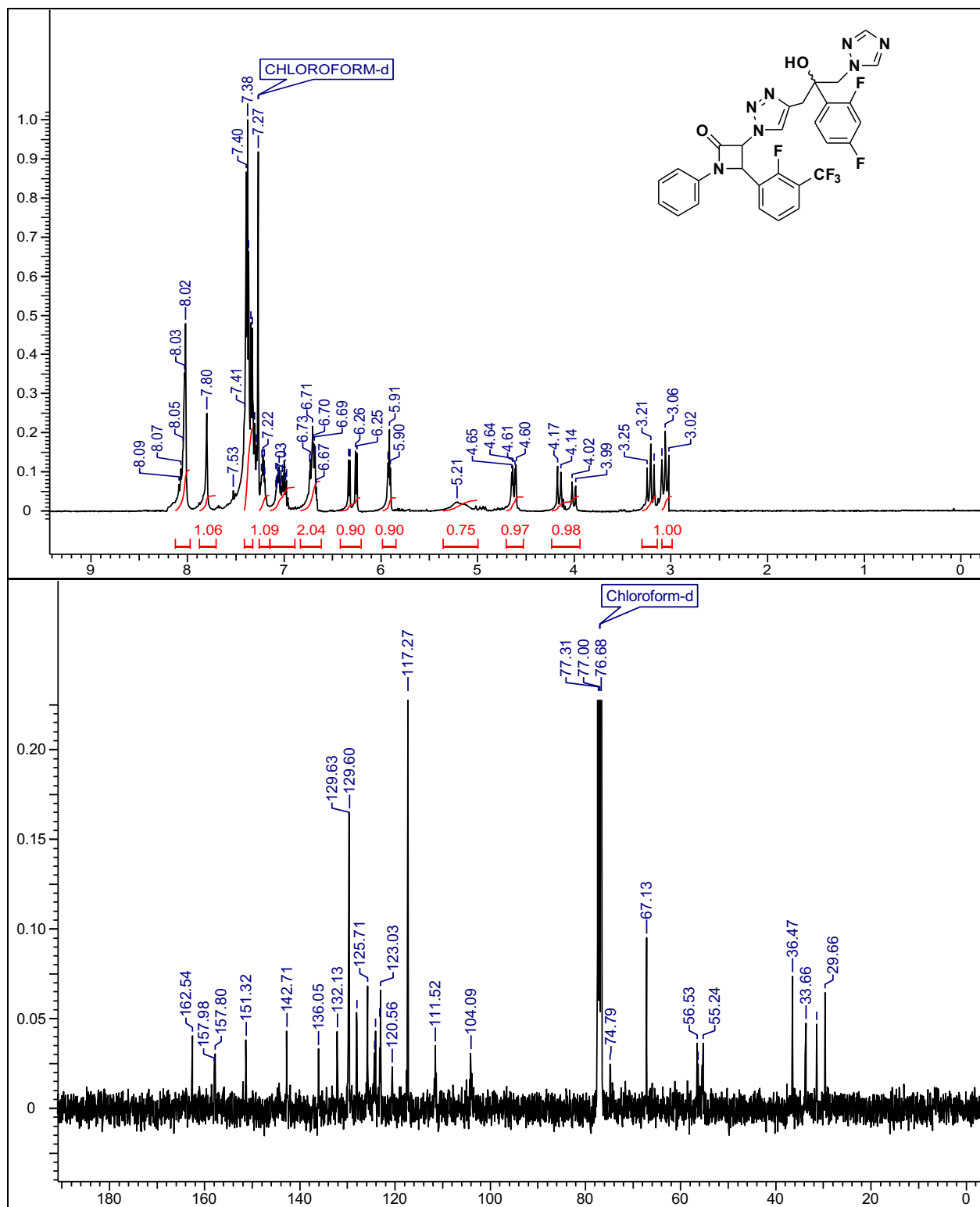
12c



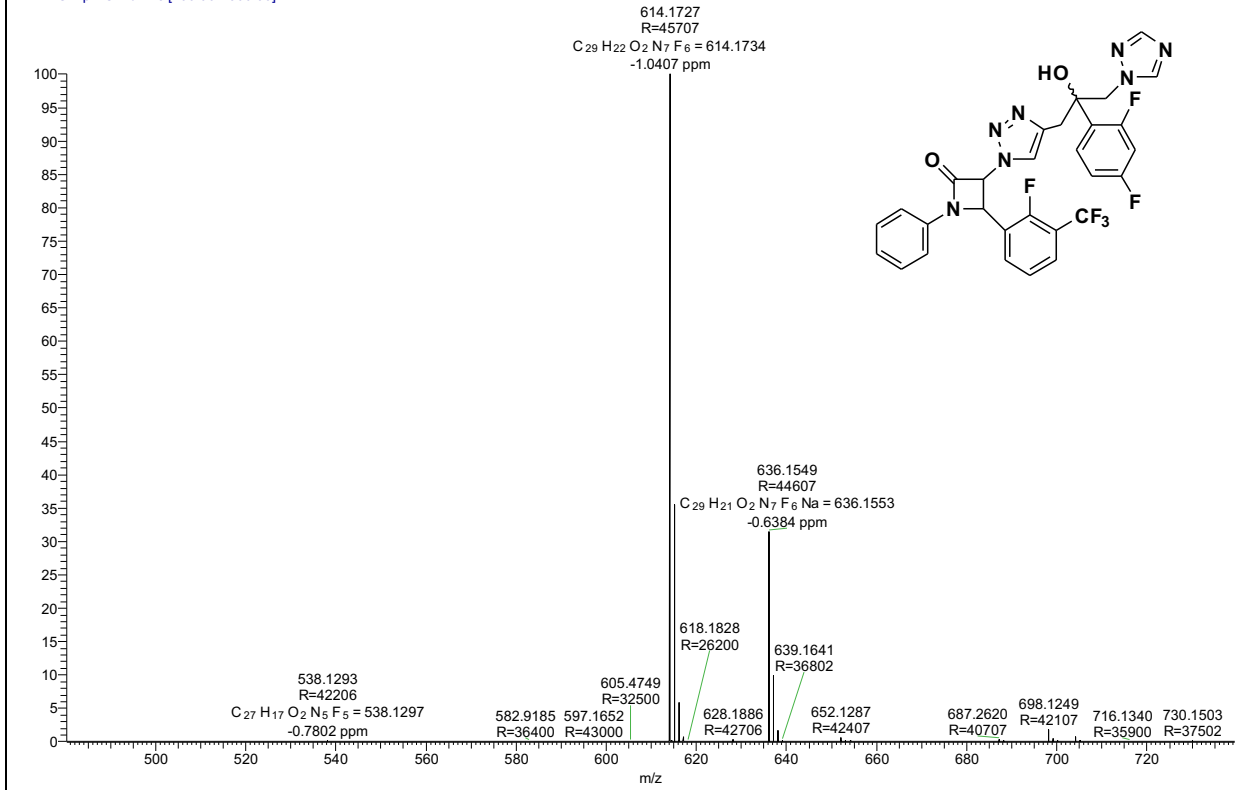


*3-(4-(2-(2,4-difluorophenyl)-2-hydroxy-3-(1*H*-1,2,4-triazol-1-yl)propyl)-1*H*-1,2,3-triazol-1-yl)-4-(2-fluoro-3-(trifluoromethyl)phenyl)-1-phenylazetidin-2-one; 12d.* Yield: 90%; IR (CHCl₃, cm⁻¹) 3415, 1761; ¹H NMR (CDCl₃, 400 MHz) δ 8.02-8.07 (m, 3H), 7.80 (s, 1H), 7.33-7.41 (m, 6H, Ar-H), 7.20-7.24 (m, 1H, Ar-H), 7.00-7.21 (m, 1H, Ar-H), 6.67-6.74 (m, 2H), 6.25-6.33 (m, 1H), 5.90-5.93 (m, 1H), 5.21 (bs, 1H), 4.60-4.65 (m, 1H), 3.99-4.17 (m, 1H), 3.17-3.25 (m, 1H), 3.02-3.10 (m, 1H); ¹³C NMR (CDCl₃, 50 MHz) δ 162.5, 158.0, 157.8, 151.3, 142.7, 136.0, 132.16, 129.6, 125.7, 123.0, 117.3, 111.5, 104.1, 74.8, 67.1, 56.5, 56.3, 55.2, 36.5, 33.7, 31.4, 29.7; ESI-MS (m/z): 614.17 [M+H]⁺; HRMS (ESI-qTOF): calcd for C₂₉H₂₂F₆N₇O₂ [M+H]⁺, 614.1734; found: 614.1727.

12d

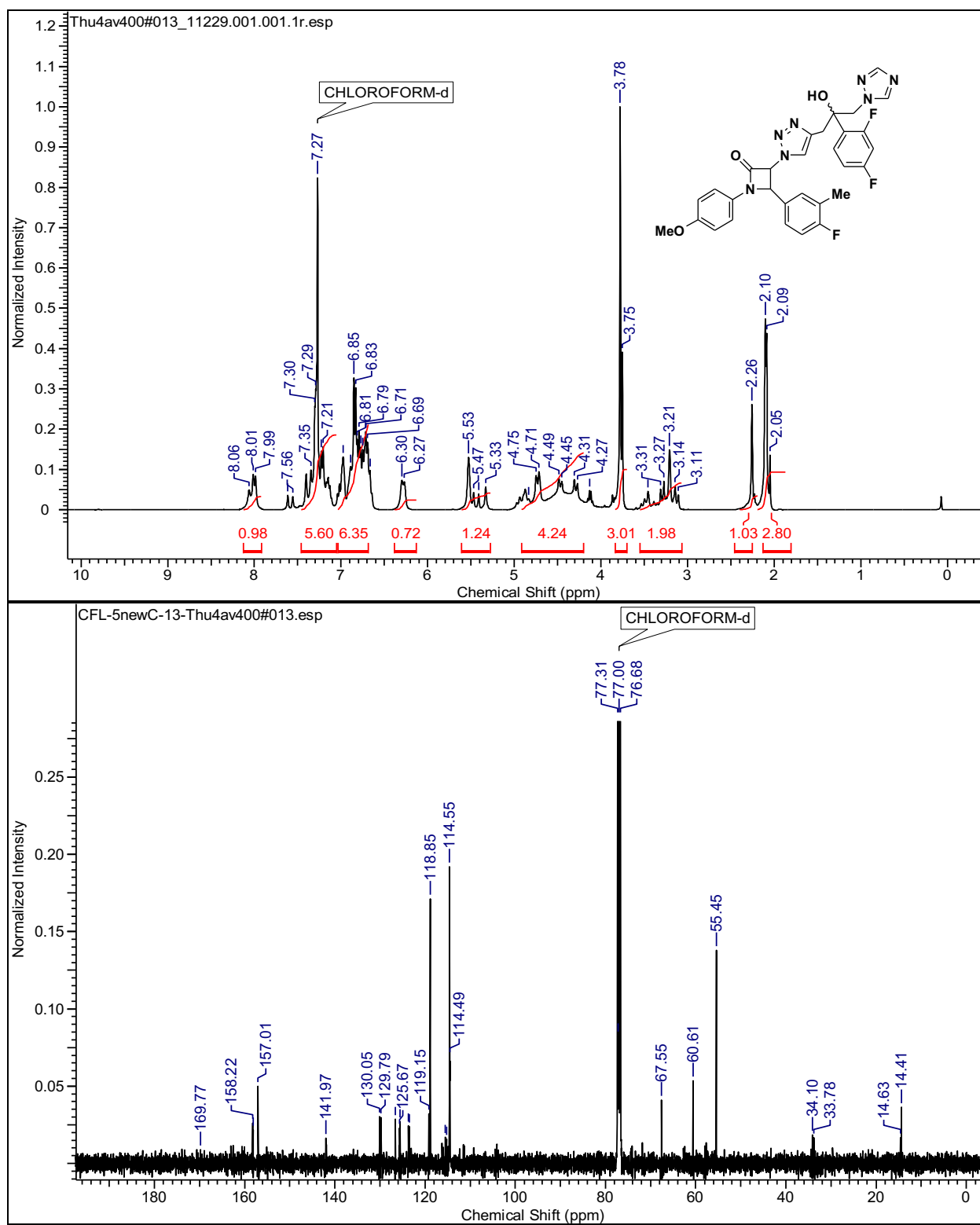


CFL-4 #98 RT: 0.43 AV: 1 NL: 1.25E9
T: FTMS + p ESI Full ms [100.00-1500.00]

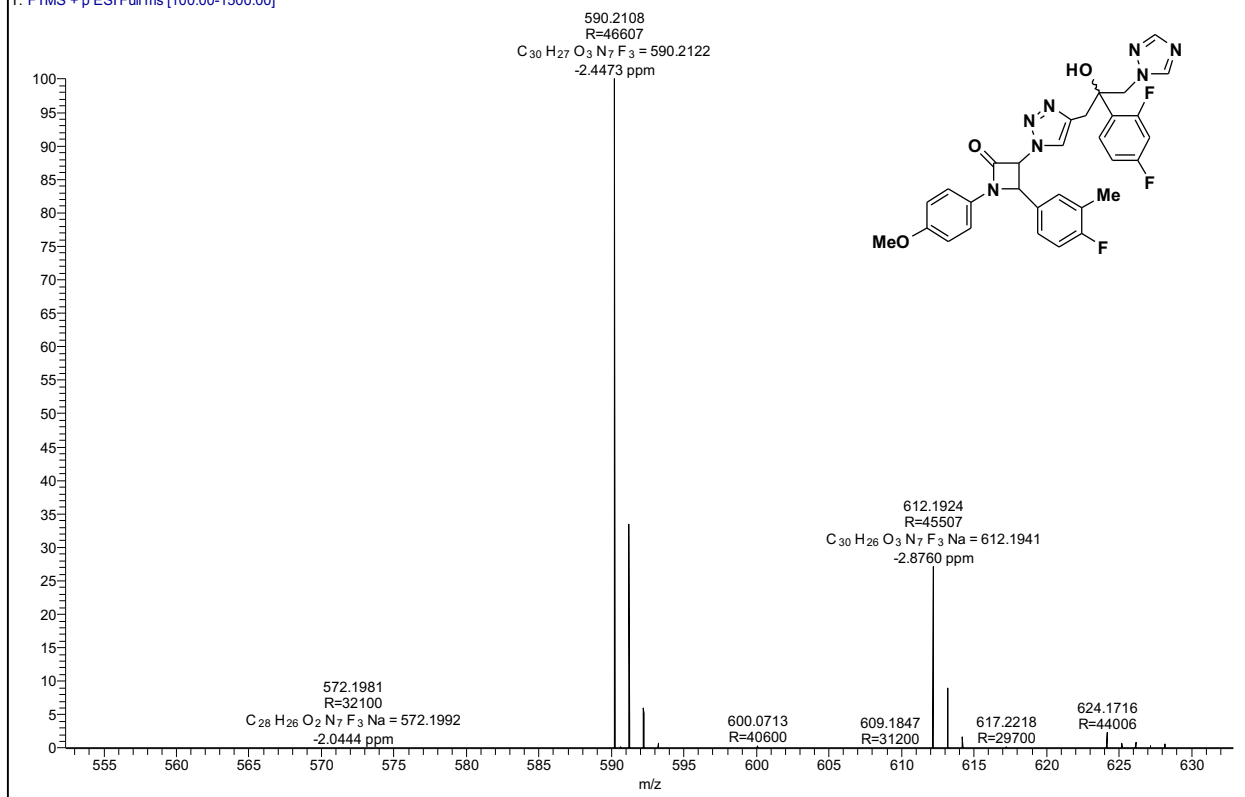


*3-(4-(2-(2,4-difluorophenyl)-2-hydroxy-3-(1*H*-1,2,4-triazol-1-yl)propyl)-1*H*-1,2,3-triazol-1-yl)-4-(4-fluoro-3-methylphenyl)-1-(4-methoxyphenyl)azetidin-2-one; 12e.* Yield: 88%; IR (CHCl_3 , cm^{-1}) 3415, 1761; ^1H NMR (CDCl_3 , 400 MHz) δ 7.99-8.06 (m, 1H), 7.15-7.40 (m, 6H), 6.67-7.02 (m, 6H), 6.29 (d, $J = 10.9$ Hz, 1H), 5.33-5.53 (m, 1H), 4.13-4.84 (m, 4H), 3.76 (m, 3H), 3.11-3.46 (m, 2H), 2.26 (s, 1H), 2.05-2.10 (m, 3H); ^{13}C NMR (CDCl_3 , 50 MHz) δ 169.7, 158.2, 157.0, 141.9, 130.0, 129.7, 126.5, 125.6, 119.1, 118.8, 115.4, 114.5, 67.5, 60.6, 55.4, 33.7, 14.6, 14.4; HRMS (ESI-qTOF): calcd for $\text{C}_{30}\text{H}_{27}\text{F}_3\text{N}_7\text{O}_3$ [$\text{M}+\text{H}]^+$, 590.2122; found: 590.2108.

12e

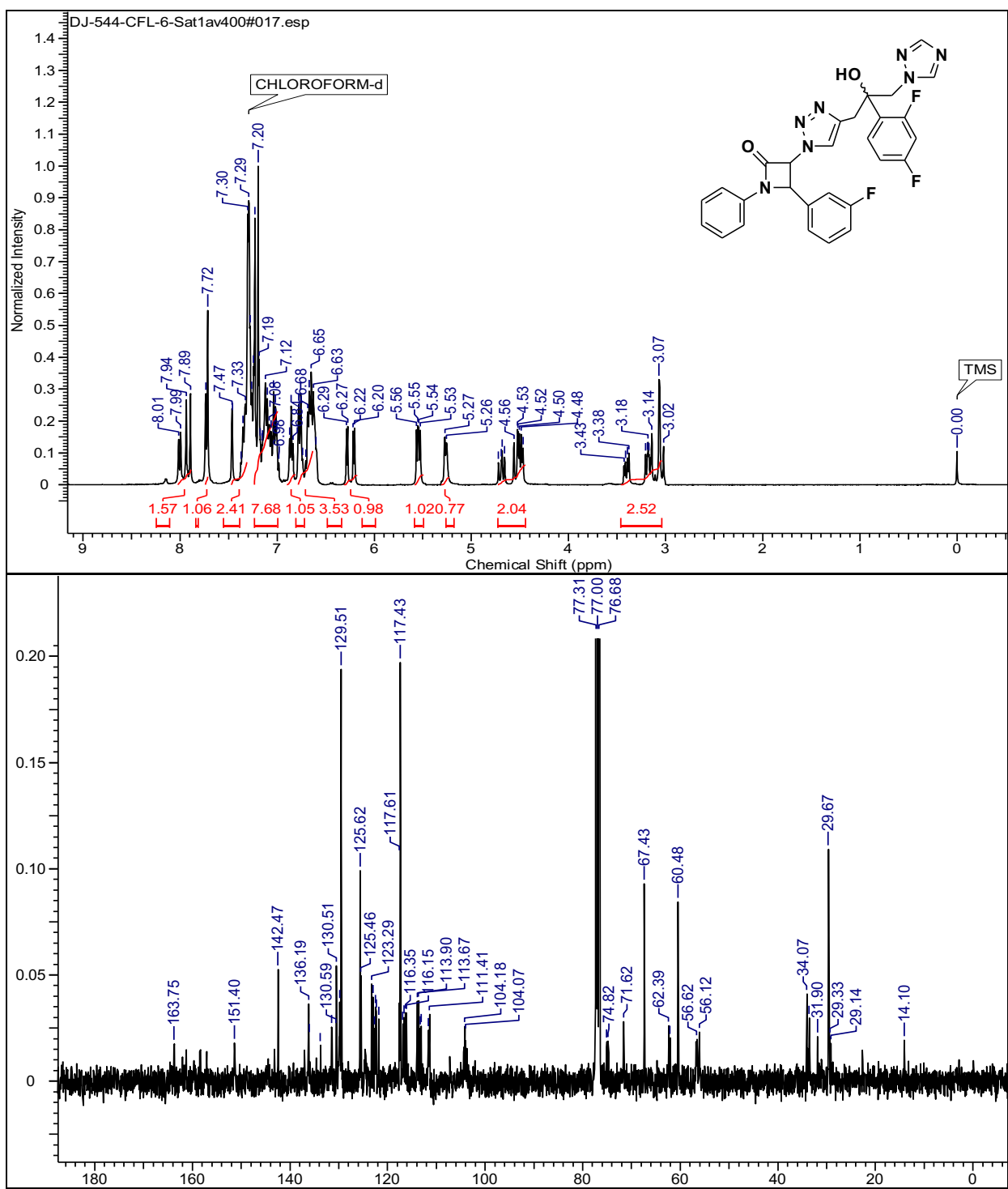


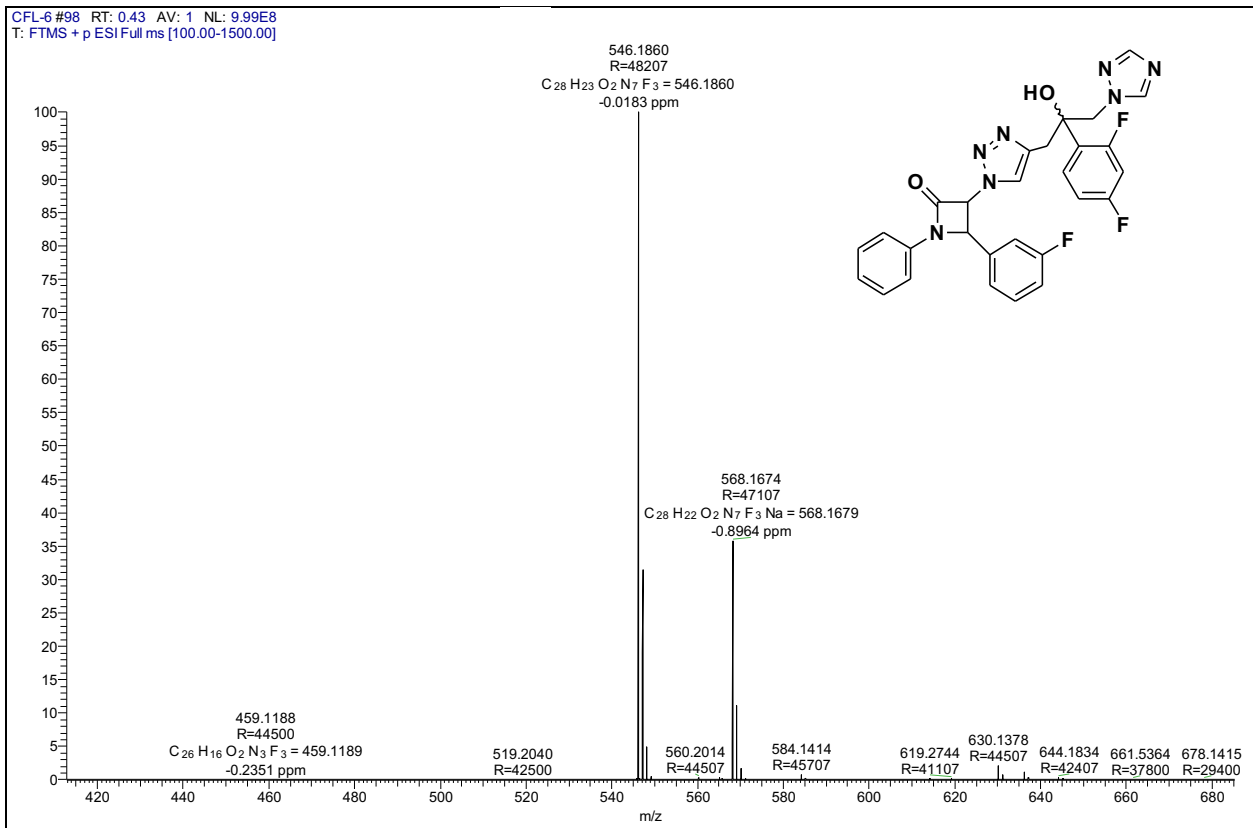
CFL-5-JAY#114 RT: 0.51 AV: 1 NL: 2.79E8
T: FTMS + p ESI Full ms [100.00-1500.00]



*3-(4-(2-(2,4-difluorophenyl)-2-hydroxy-3-(1*H*-1,2,4-triazol-1-yl)propyl)-1*H*-1,2,3-triazol-1-yl)-4-(3-fluorophenyl)-1-phenylazetidin-2-one; 12f.* Yield: 91%; semi-solid; IR (CHCl_3 , cm^{-1}) 3415, 1761; ^1H NMR (CDCl_3 , 400 MHz) δ 7.89-8.01 (m, 1H), 7.73 (d, $J = 7.82$ Hz, 1H), 7.30-7.37 (m, 2H, Ar-H), 7.0-7.24 (m, 7H, Ar-H), 6.84-6.87 (m, 1H, Ar-H), 6.63-6.78(m, 3H), 6.20-6.29 (m, 1H), 5.53-5.56 (m, 1H), 5.26 (bs, 1H), 4.47-4.72 (m, 2H), 3.02-3.43 (m, 2H); ^{13}C NMR (CDCl_3 , 50 MHz) δ 163.7, 161.2, 158.5, 158.4, 154.3, 151.4, 144.2, 142.4, 136.2, 130.4, 129.8, 129.5, 125.6, 123.2, 117.4, 116.3, 113.8, 111.5, 104.1, 75.1, 74.8, 67.4, 60.4, 56.5, 534.1, 33.9, 29.6, 21.0, 14.1. ESI-MS (m/z): 546.18 [$M+H]^+$; HRMS (ESI-qTOF): calcd for $C_{28}H_{23}F_3N_7O_3$ [$M+H]^+$, 546.1860; found: 546.1860.

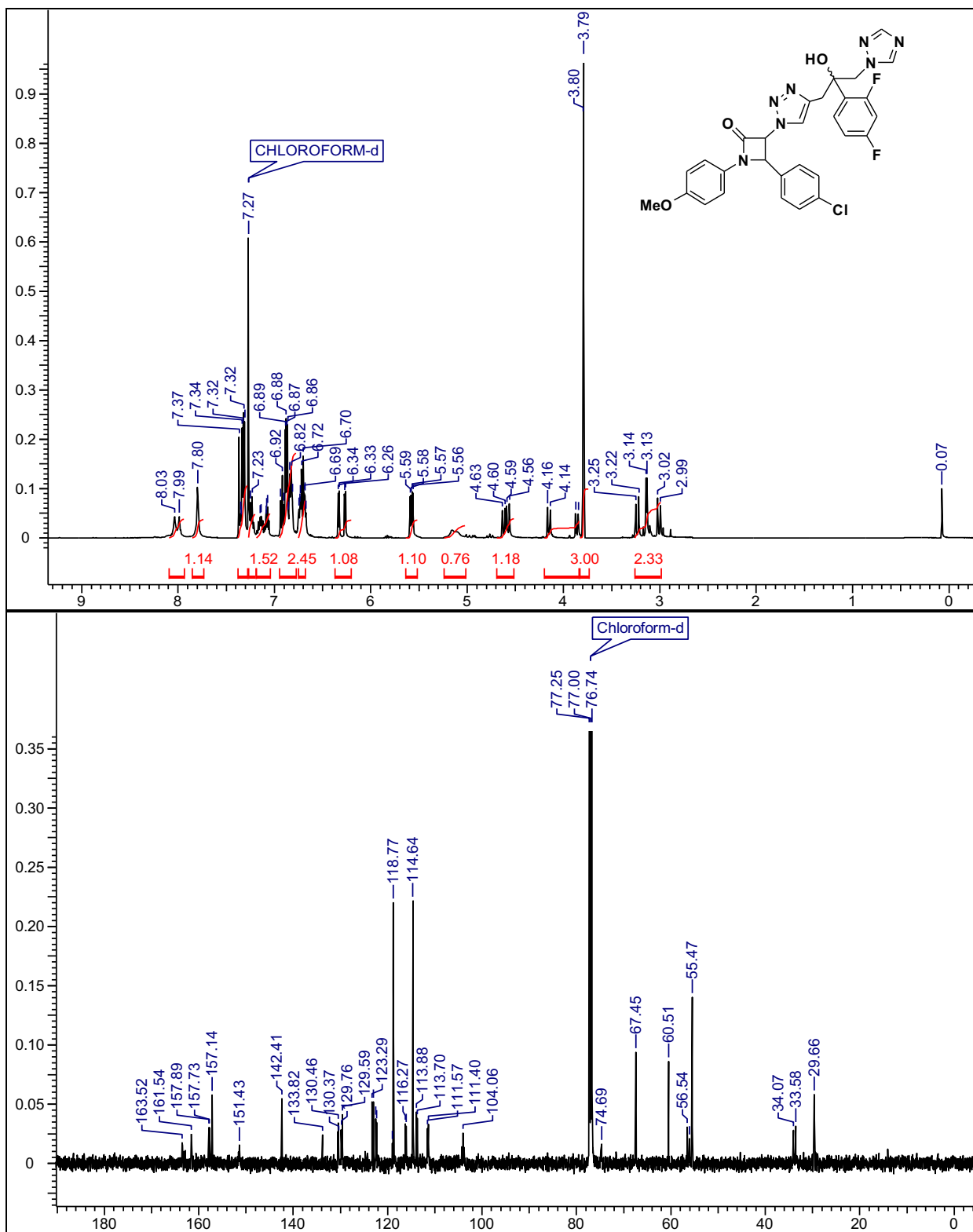
12f



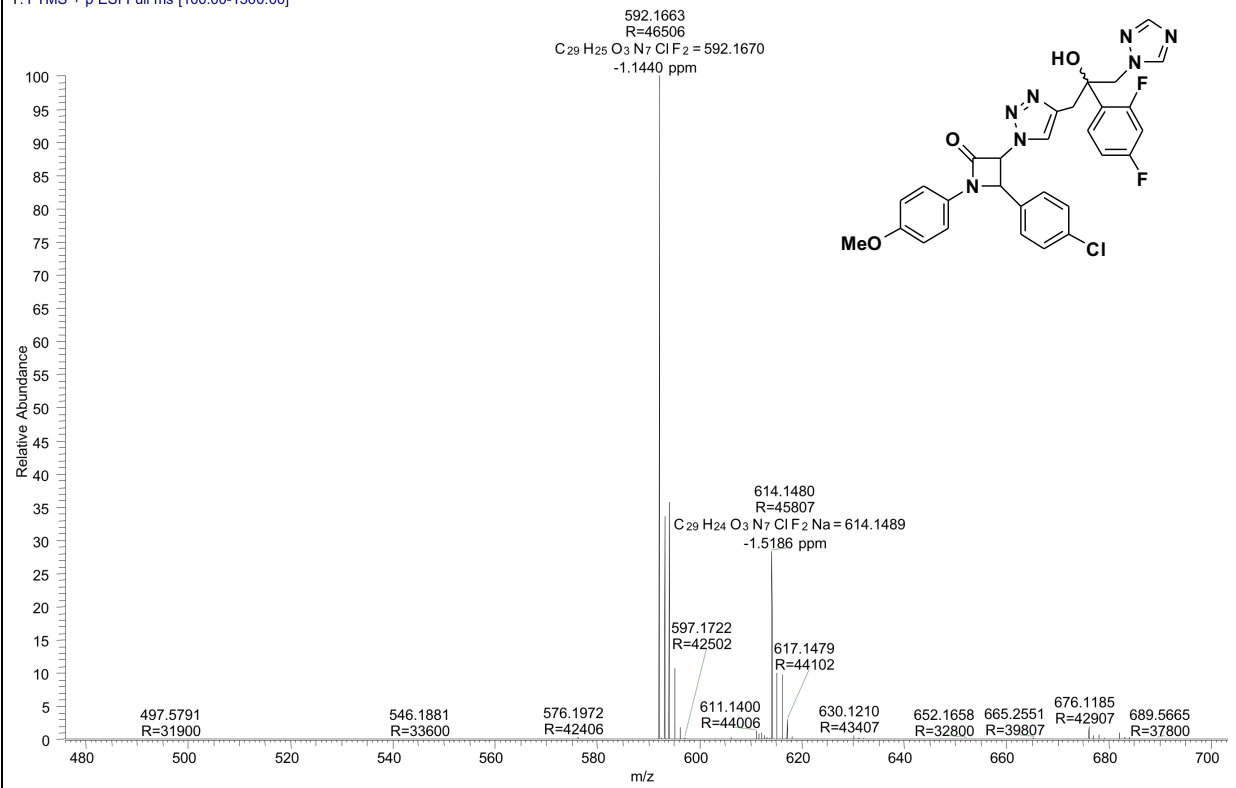


*4-(4-chlorophenyl)-3-(4-(2,4-difluorophenyl)-2-hydroxy-3-(1*H*-1,2,4-triazol-1-yl)propyl)-1*H*-1,2,3-triazol-1-yl-1-(4-methoxyphenyl)azetidin-2-one; **12g**.* Yield: 90%; IR (CHCl₃, cm⁻¹) 3415, 1761; ¹H NMR (CDCl₃, 500 MHz) δ 7.99-8.03 (m, 1H), 7.80 (s, 1H), 7.31-7.37 (m, 3H, Ar-H), 7.23-7.26 (m, 1H, Ar-H), 7.07-7.15 (m, 1H), 6.81-6.93 (m, 5H), 6.68-6.74 (m, 2H), 6.26-6.34 (m, 1H), 5.56-5.59 (m, 1H), 5.15 (bs, 1H), 4.56-4.63 (m, 1H), 3.87-4.16 (m, 1H), 3.80 (s, 3H), 2.99-3.25 (m, 2H); ¹³C NMR (CDCl₃, 50 MHz) δ 163.5, 161.5, 157.8, 157.1, 151.4, 142.4, 133.8, 130.4, 129.7, 129.5, 123.2, 122.4, 118.7, 114.6, 113.8, 113.7, 111.5, 111.4, 104.0, 74.6, 67.45, 60.5, 66.5, 55.4, 34.0, 33.5, 29.6; ESI-MS (m/z): 592.14 [M+H]⁺; HRMS (ESI-qTOF): calcd for C₂₉H₂₅ClF₂N₇O₃ [M+H]⁺, 592.1670; found: 592.1663.

12g

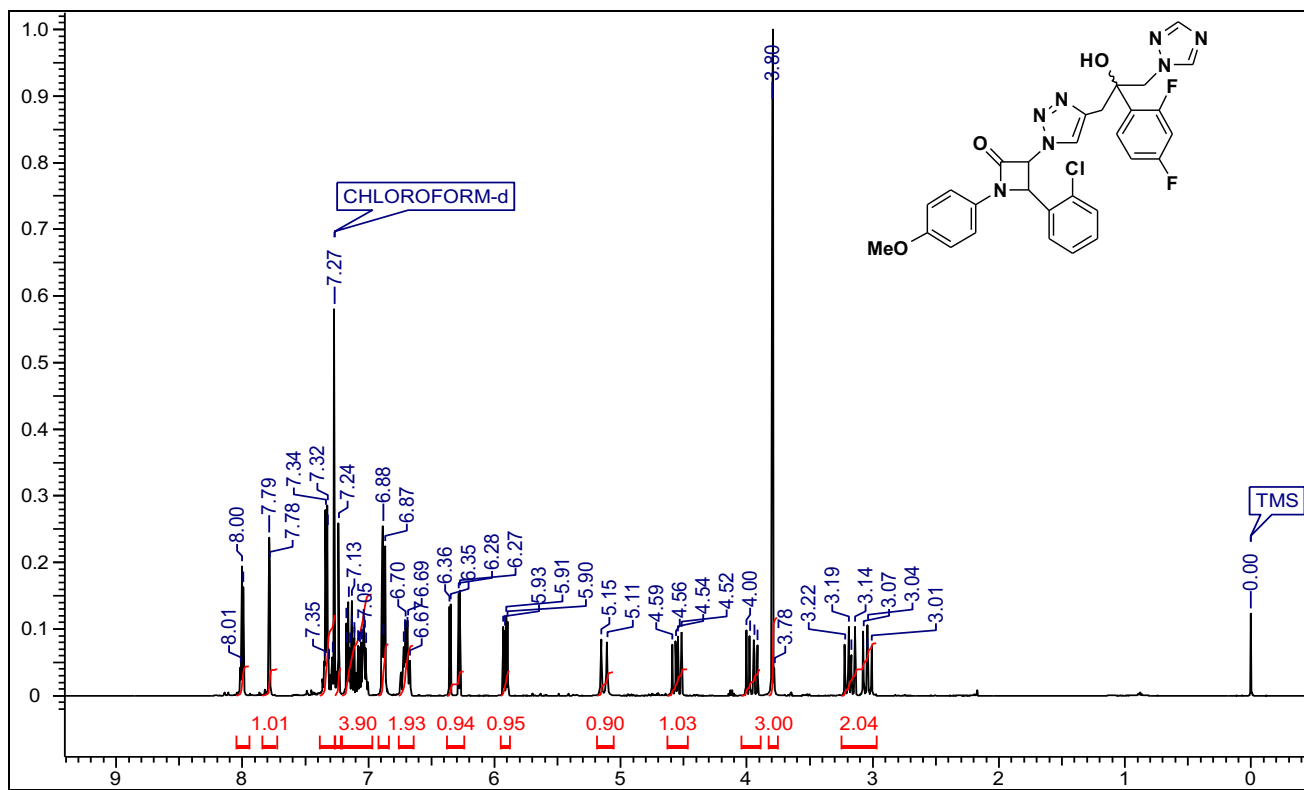


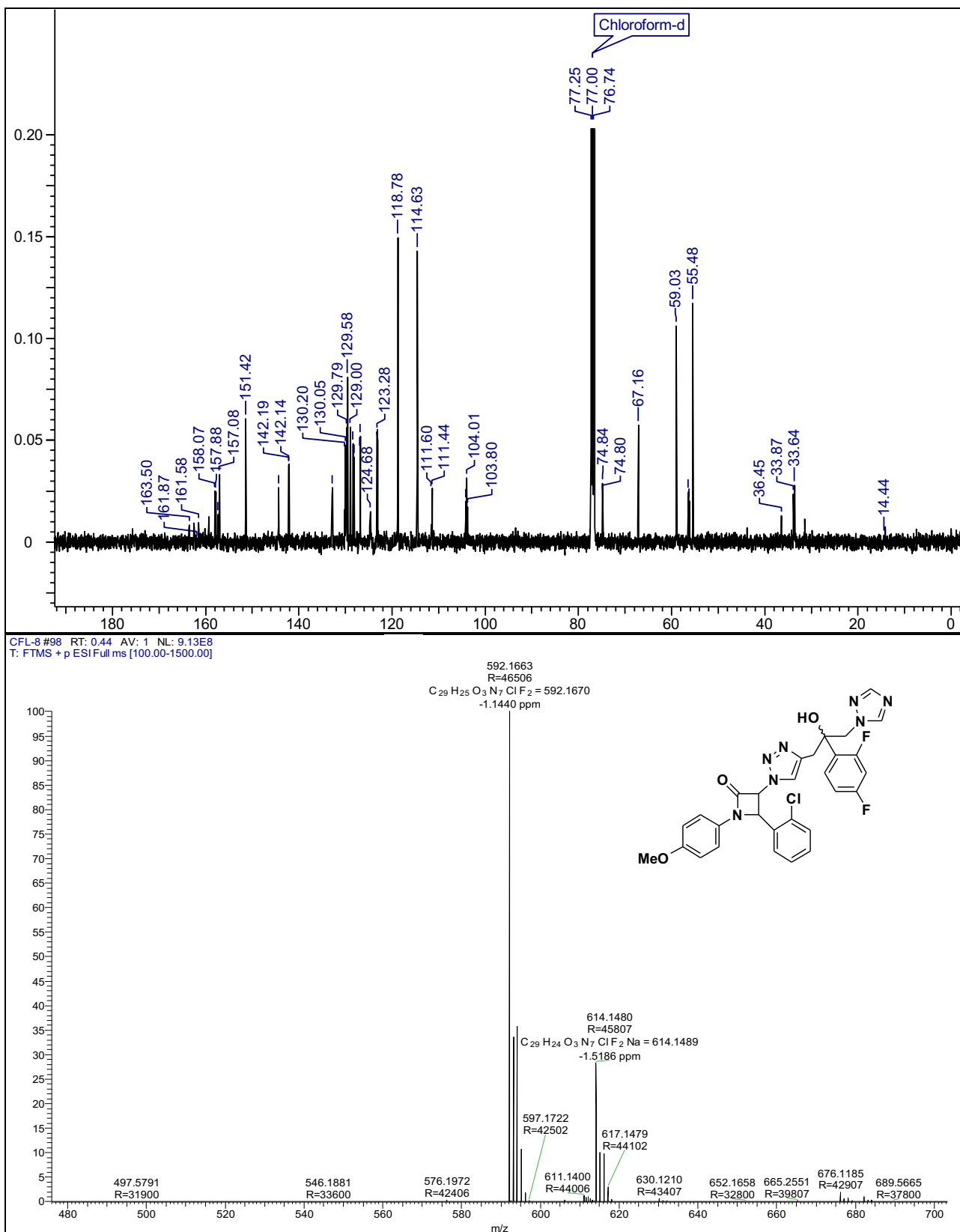
CFL-7#98 RT: 0.44 AV: 1 NL: 9.13E8
T: FTMS + p ESI Full ms [100.00-1500.00]



*4-(2-chlorophenyl)-3-(4-(2,4-difluorophenyl)-2-hydroxy-3-(1*H*-1,2,4-triazol-1-yl)propyl)-1*H*-1,2,3-triazol-1-yl-1-(4-methoxyphenyl)azetidin-2-one; 12h.* Yield: 92%; IR (CHCl_3 , cm^{-1}) 3415, 1761; ^1H NMR (CDCl_3 , 500 MHz) δ 7.99-8.01 (m, 1H), 7.79 (s, 1H), 7.28-7.35 (m, 3H, Ar-H), 7.23-7.24 (m, 1H, Ar-H), 7.02-7.17 (m, 4H), 6.87-6.89 (m, 2H), 6.67-6.72 (m, 2H), 6.27-6.36 (m, 1H), 5.90-5.93 (m, 1H), 5.13 (bs, 1H), 4.52-4.59 (m, 1H), 3.91-4.0 (m, 1H), 3.80 (s, 3H), 3.01-3.22 (m, 2H); ^{13}C NMR (CDCl_3 , 50 MHz) δ 163.5, 161.8, 161.5, 158.0, 157.8, 157.1, 151.4, 142.4, 132.8, 130.0, 129.7, 129.5, 128.4, 123.2, 122.4, 118.7, 114.6, 113.8, 113.7, 111.5, 111.4, 104.0, 74.6, 74.8, 67.45, 59.0, 56.4, 56.2, 36.4, 33.8, 14.4; ESI-MS (m/z): 592.14 [$\text{M}+\text{H}]^+$; HRMS (ESI-qTOF): calcd for $\text{C}_{29}\text{H}_{25}\text{ClF}_2\text{N}_7\text{O}_3$ [$\text{M}+\text{H}]^+$, 592.1670: found: 592.1663.

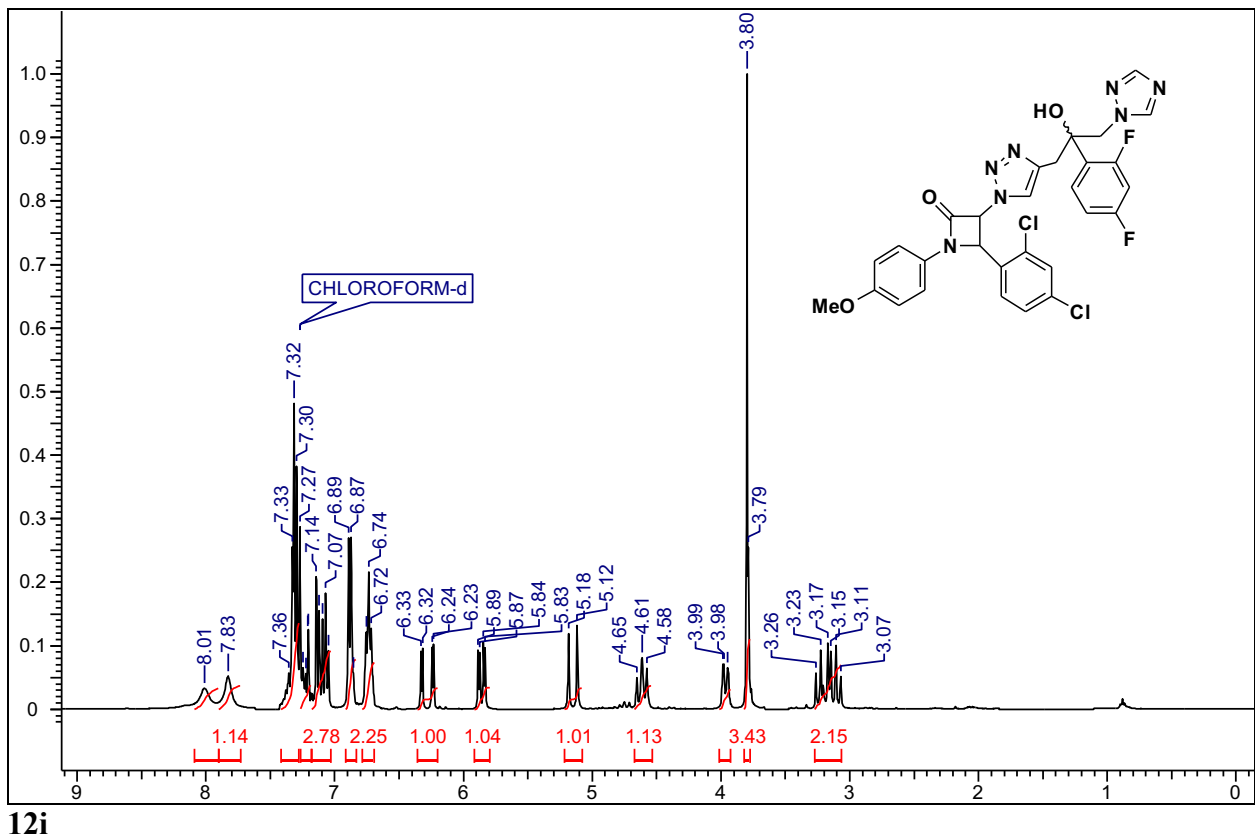
12h

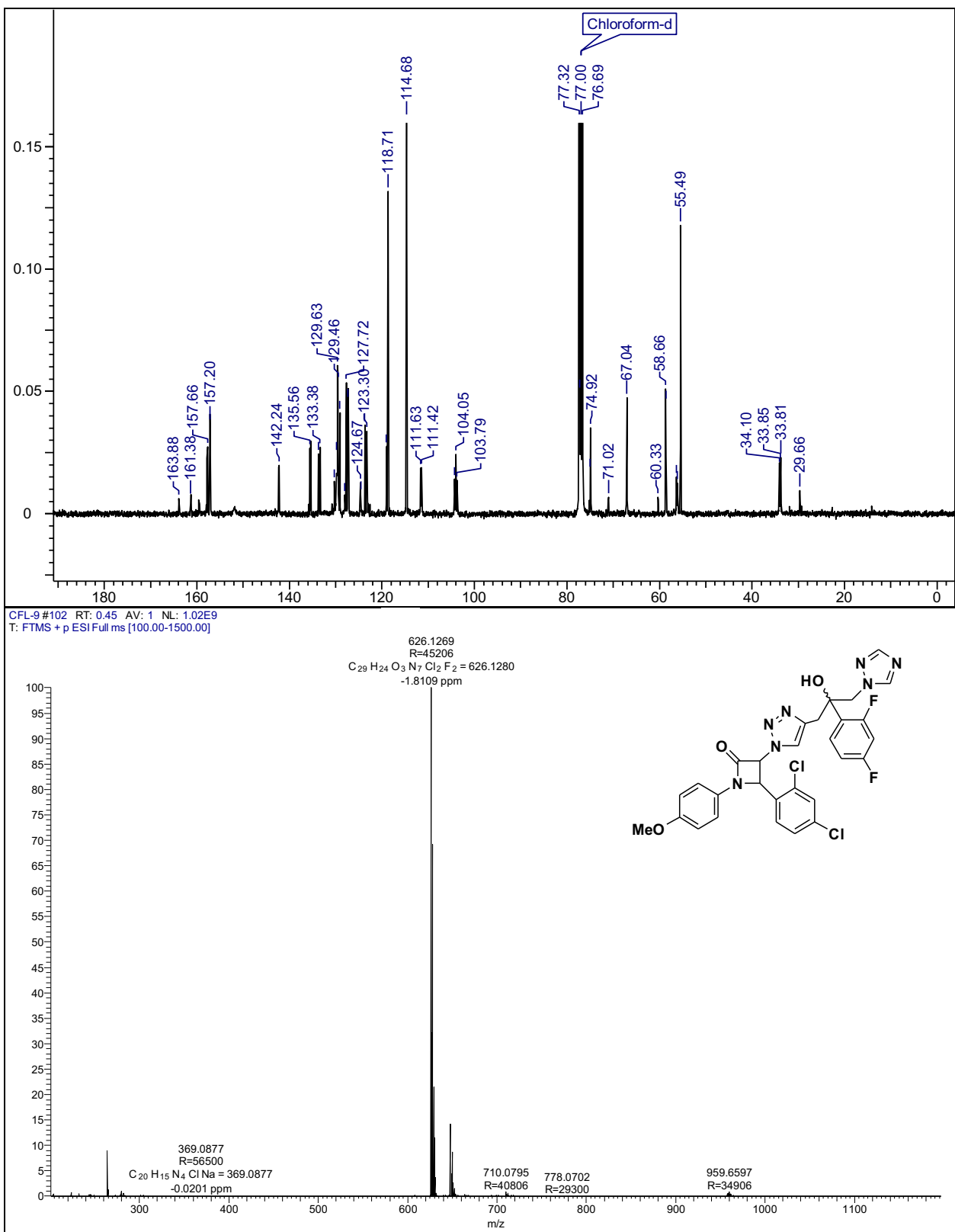




*4-(2,4-dichlorophenyl)-3-(4-(2,4-difluorophenyl)-2-hydroxy-3-(1*H*-1,2,4-triazol-1-yl)propyl)-1*H*-1,2,3-triazol-1-yl)-1-(4-methoxyphenyl)azetidin-2-one; **12i**.* Yield: 90%; IR (CHCl₃, cm⁻¹) 3415, 1761; ¹H NMR (CDCl₃, 400 MHz) δ 8.01 (s, 1H), 7.83 (s, 1H), 7.30-7.36 (m, 4H, Ar-H), 7.21-7.25 (m, 1H, Ar-H), 7.05-7.14 (m, 2H), 6.86-6.90 (m, 2H), 6.72-6.76 (m, 2H), 6.23-6.33 (m, 1H), 5.83-5.89 (m, 1H), 5.14 (bs, 1H), 4.58-4.65 (m, 1H), 3.95-3.99 (m, 1H), 3.80 (s, 3H), 3.07-3.26 (m, 2H); ¹³C NMR (CDCl₃, 50 MHz) δ 163.8, 161.3, 161.2, 157.8, 157.6, 157.1, 142.2, 165.5, 135.4, 129.7, 129.6, 127.7, 127.2, 118.7, 114.6, 111.6, 111.4, 104.3, 103.7, 74.9, 71.0, 67.0, 60.3, 58.6, 58.5, 55.4, 34.1, 33.8, 29.6; ESI-MS (m/z): 626.14 [M+H]⁺; HRMS (ESI-qTOF): calcd for C₂₉H₂₄Cl₂F₂N₇O₃ [M+H]⁺, 626.1280; found: 626.1269.

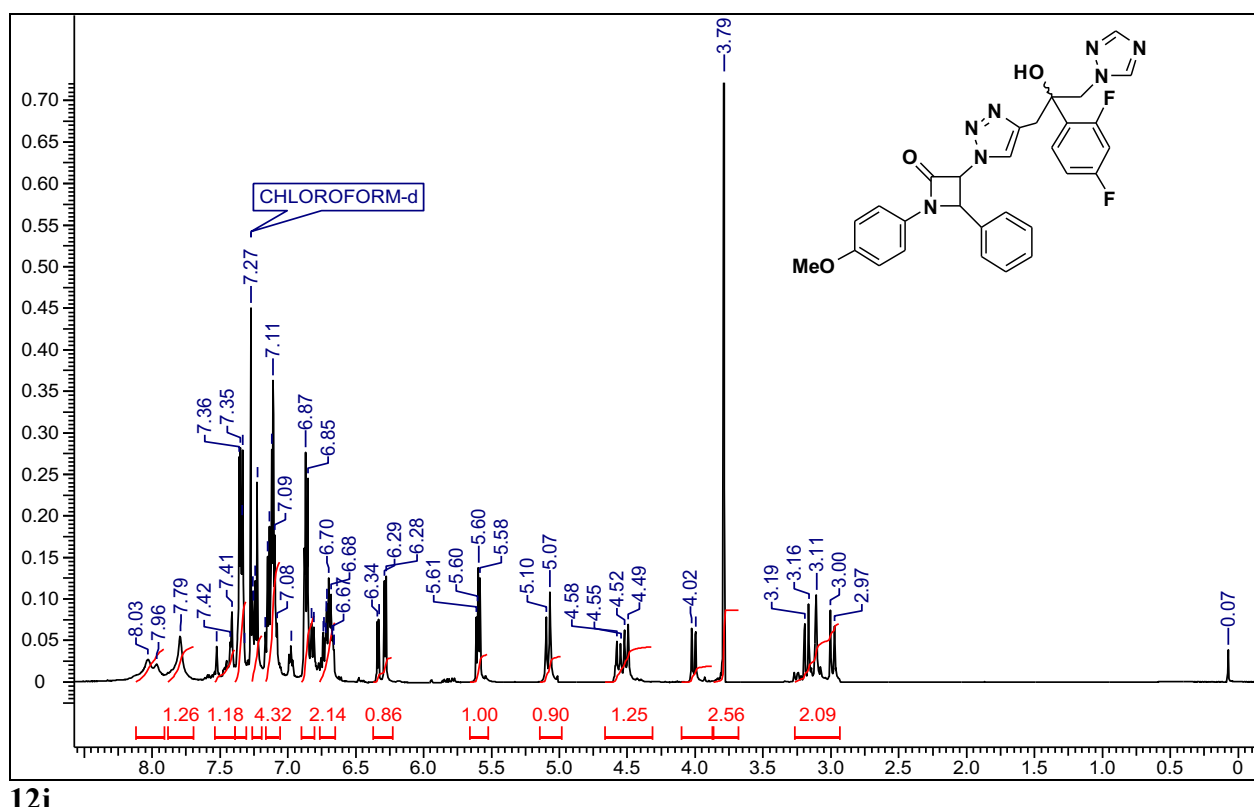
12i

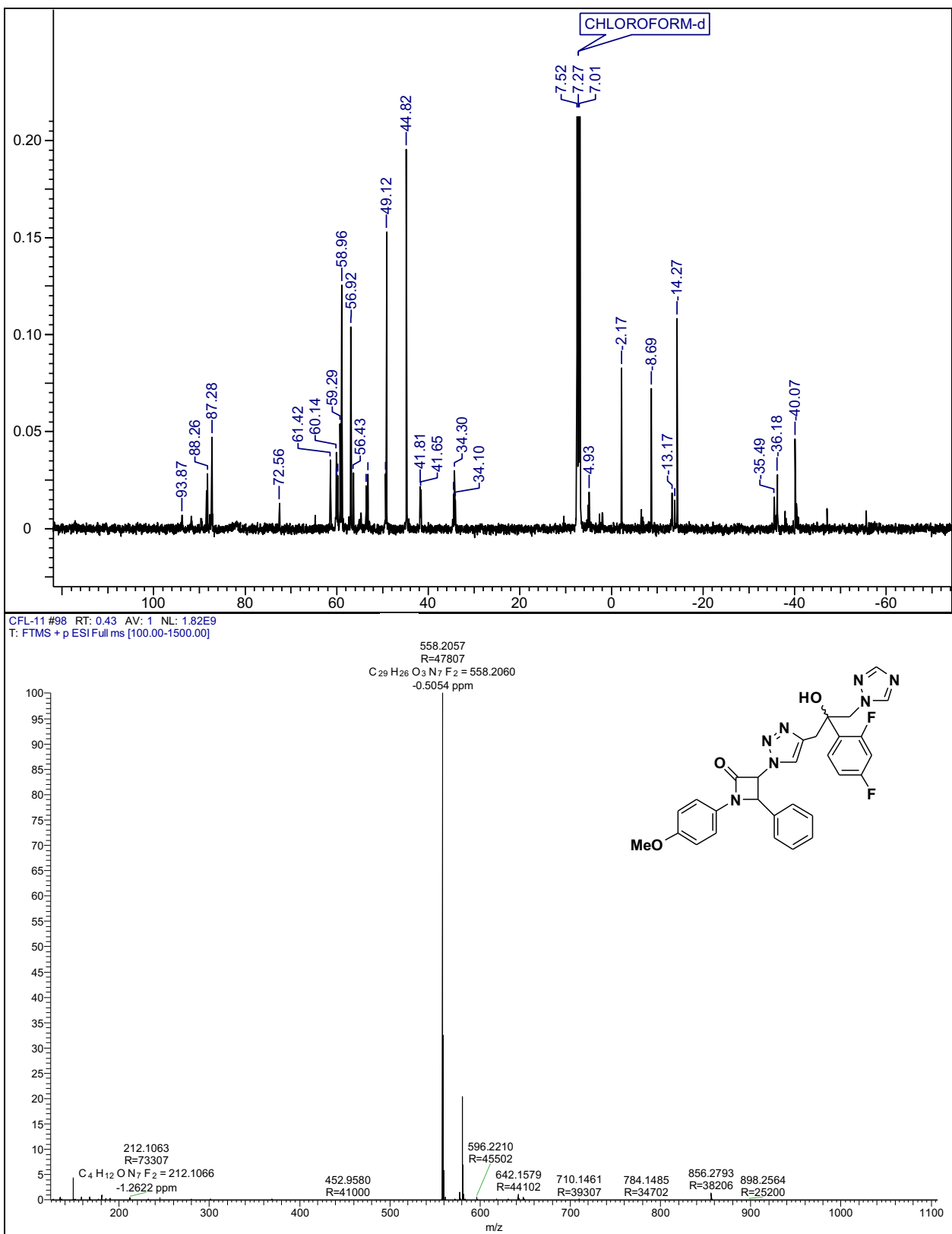




*3-(4-(2,4-difluorophenyl)-2-hydroxy-3-(1*H*-1,2,4-triazol-1-yl)propyl)-1*H*-1,2,3-triazol-1-yl)-1-(4-methoxyphenyl)-4-phenylazetidin-2-one; **12j**.* Yield: 90%; IR (CHCl₃, cm⁻¹) 3415, 1761; ¹H NMR (CDCl₃, 500 MHz) δ 7.96-8.03 (m, 1H), 7.79 (s, 1H), 7.41-7.52 (m, 1H), 7.33-7.35 (m, 2H, Ar-H), 7.22-7.26 (m, 1H, Ar-H), 7.07-7.16 (m, 4H), 6.80-6.87 (m, 2H), 6.66-6.74 (m, 2H), 6.28-6.34 (m, 1H), 5.58-5.61 (m, 1H), 5.07 (bs, 1H), 4.49-4.58 (m, 1H), 4.0-4.02 (m, 1H), 3.78 (s, 3H), 2.97-3.19 (m, 2H); ¹³C NMR (CDCl₃, 50 MHz) δ 163.6, 158.1, 157.9, 157.0, 142.2, 131.1, 129.8, 129.0, 128.6, 126.6, 126.5, 126.1, 119.0, 118.8, 114.5, 114.4, 111.5, 111.3, 104.0, 103.8, 74.6, 67.5, 61.04, 56.5, 55.9, 55.4, 34.2, 29.6; ESI-MS (m/z): 558.18 [M+H]⁺; HRMS (ESI-qTOF): calcd for C₂₉H₂₆F₂N₇O₃ [M+H]⁺, 558.2060; found: 558.2057.

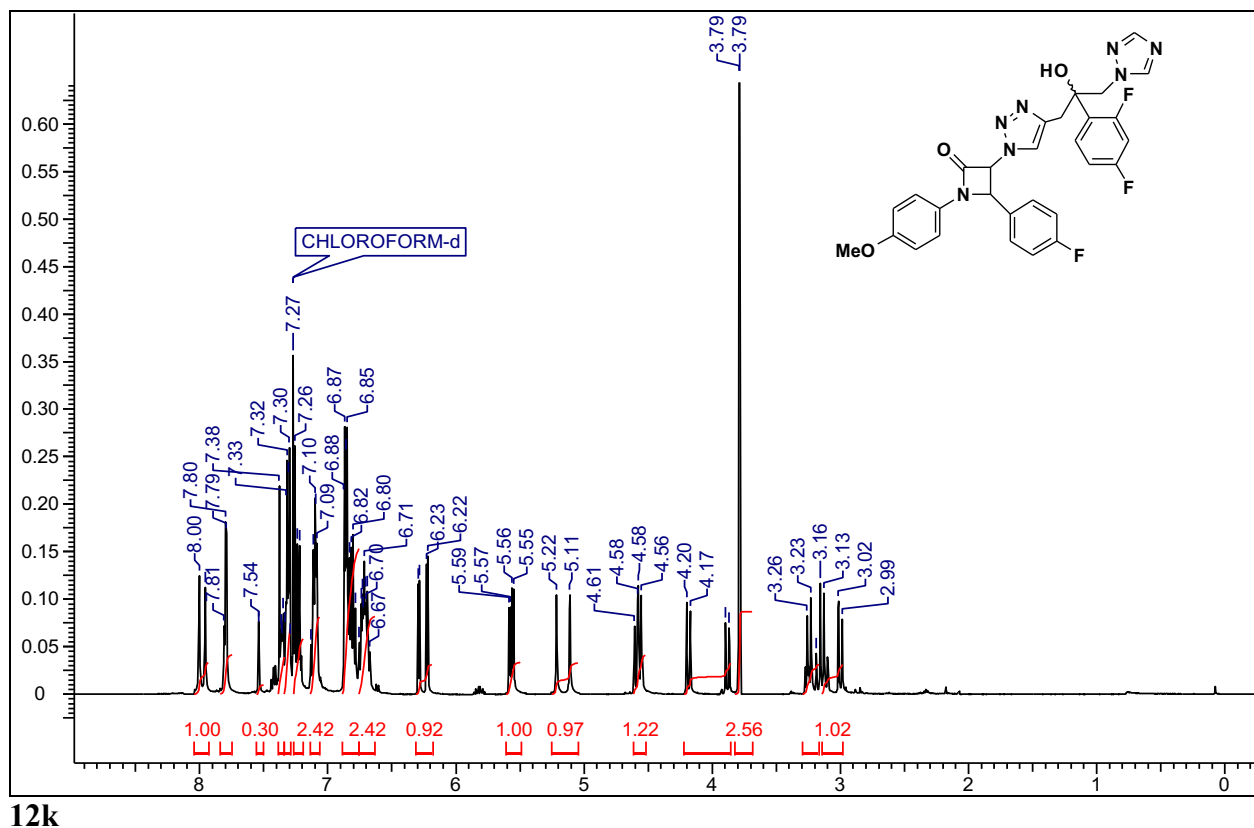
12j

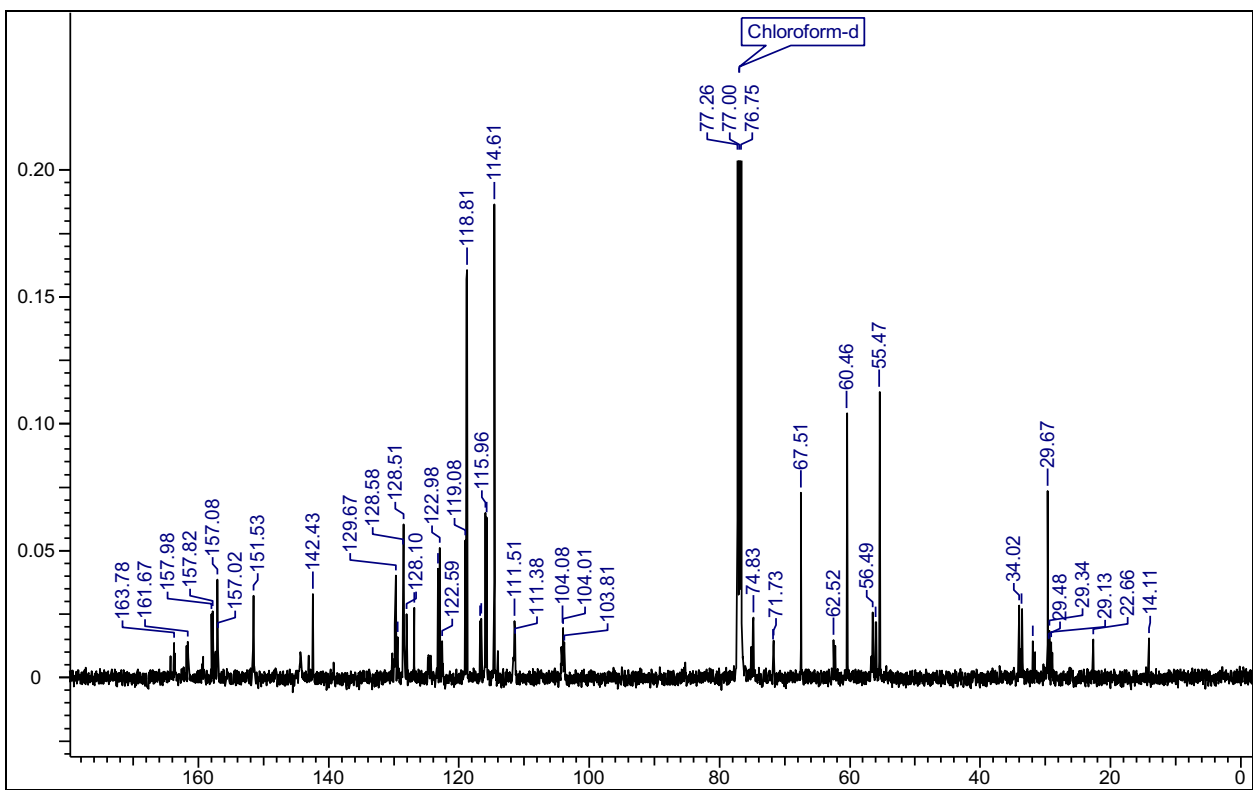




*3-(4-(2,4-difluorophenyl)-2-hydroxy-3-(1*H*-1,2,4-triazol-1-yl)propyl)-1*H*-1,2,3-triazol-1-yl)-4-(4-fluorophenyl)-1-(4-methoxyphenyl)azetidin-2-one; **12k**.* Yield: 93%; semi-solid; IR (CHCl₃, cm⁻¹) 3415, 1761; ¹H NMR (CDCl₃, 500 MHz) δ 7.96-8.0 (m, 1H), 7.79-7.81 (m, 1H), 7.35-7.38 (m, 1H), 7.29-7.33 (m, 2H, Ar-H), 7.22-7.26 (m, 2H, Ar-H), 7.09-7.13 (m, 2H), 6.80-6.88 (m, 4H), 6.67-6.78 (m, 2H), 6.22-6.29 (m, 1H), 5.55-5.59 (m, 1H), 5.11 (bs, 1H), 4.56-4.61 (m, 1H), 3.87-4.20 (m, 1H), 3.79 (s, 3H), 3.19-3.26 (m, 1H), 2.99-3.13 (m, 1H); ¹³C NMR (CDCl₃, 50 MHz) δ 163.7, 163.6, 161.6, 157.8, 151.5, 142.4, 129.6, 128.5, 126.9, 123.2, 122.9, 119.0, 118.8, 115.9, 115.7, 114.6, 111.5, 104.0, 74.9, 74.8, 67.5, 62.5, 60.4, 56.4, 34.0, 29.6, 14.1; ESI-MS (m/z): 576.19 [M+H]⁺; HRMS (ESI-qTOF): calcd for C₂₉H₂₅F₃N₇O₃ [M+H]⁺, 576.1965; found: 576.1968.

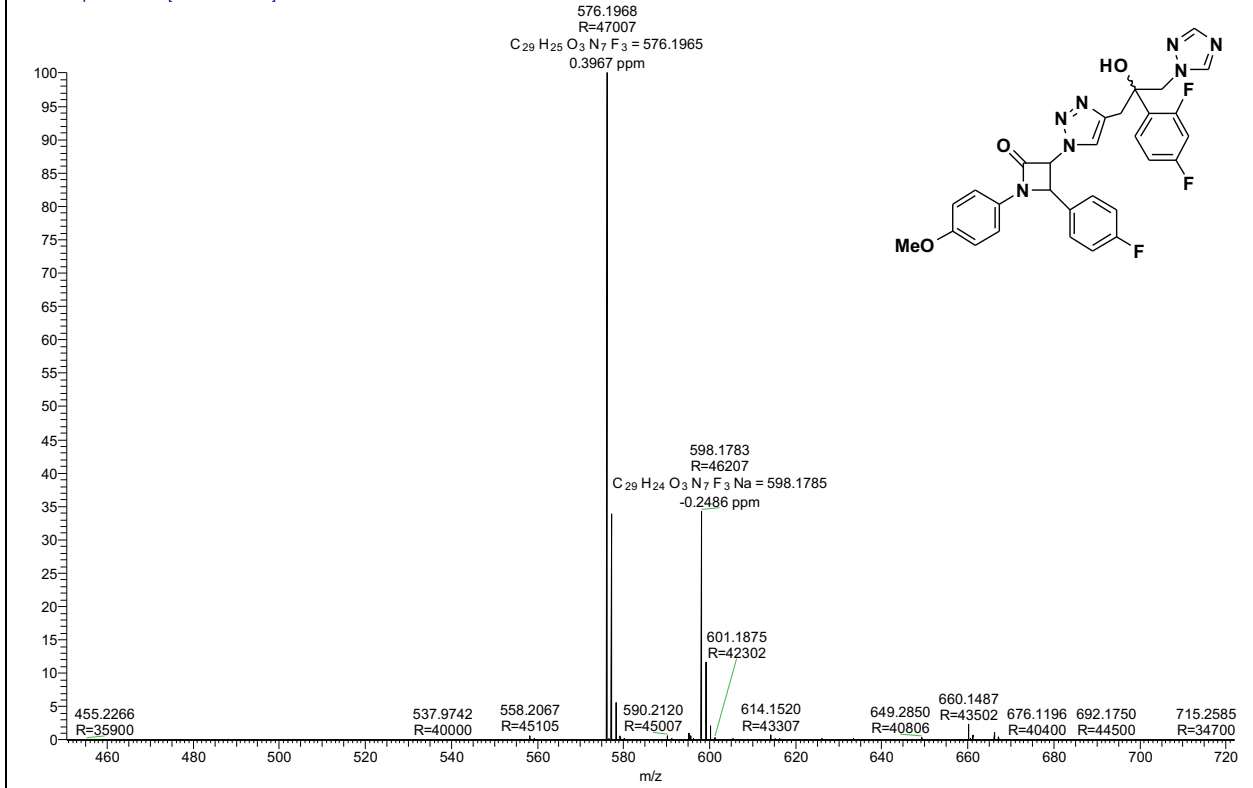
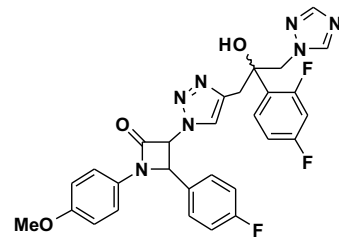
12k





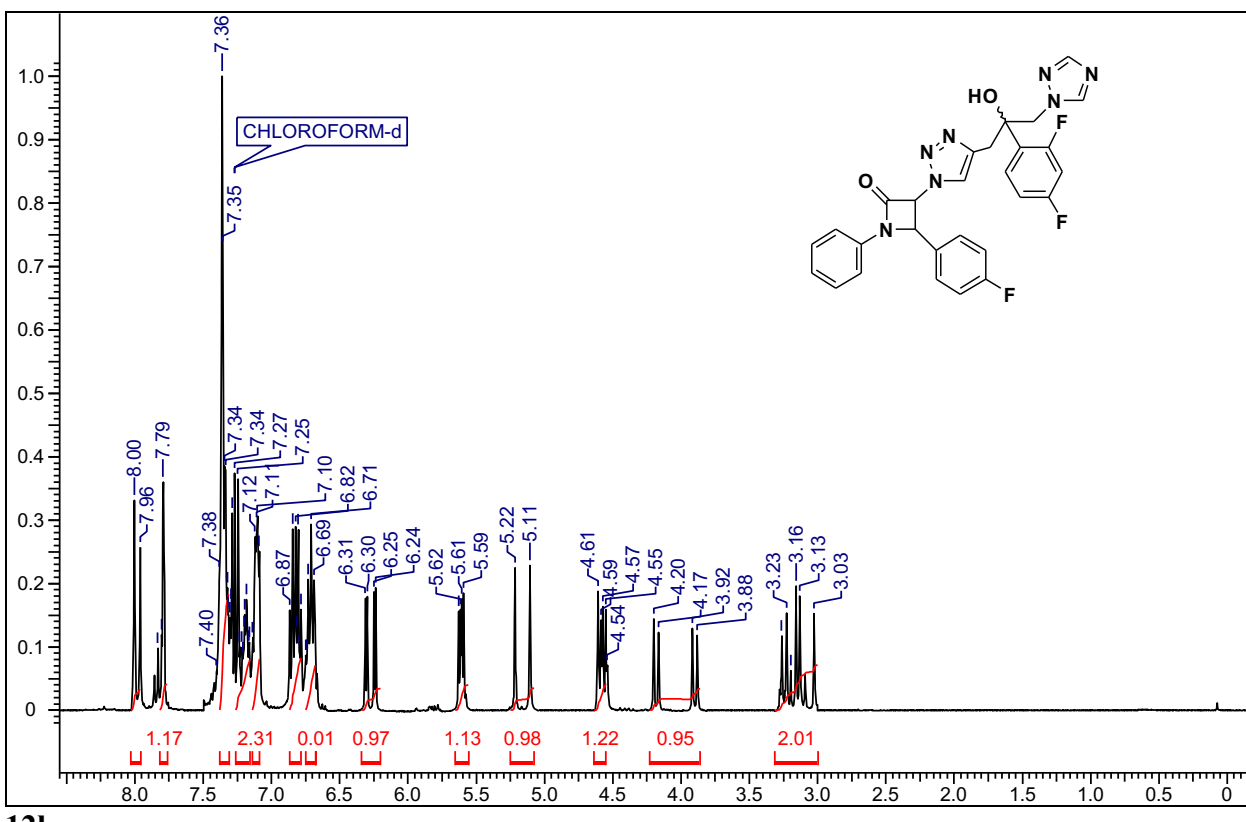
CFL-12 #97 RT: 0.43 AV: 1 NL: 9.69E8
T: FTMS + p ESI Full ms [100.00-1500.00]

576.1968
R=47007
 $C_{29}H_{25}O_3N_7F_3 = 576.1965$
0.3967 ppm

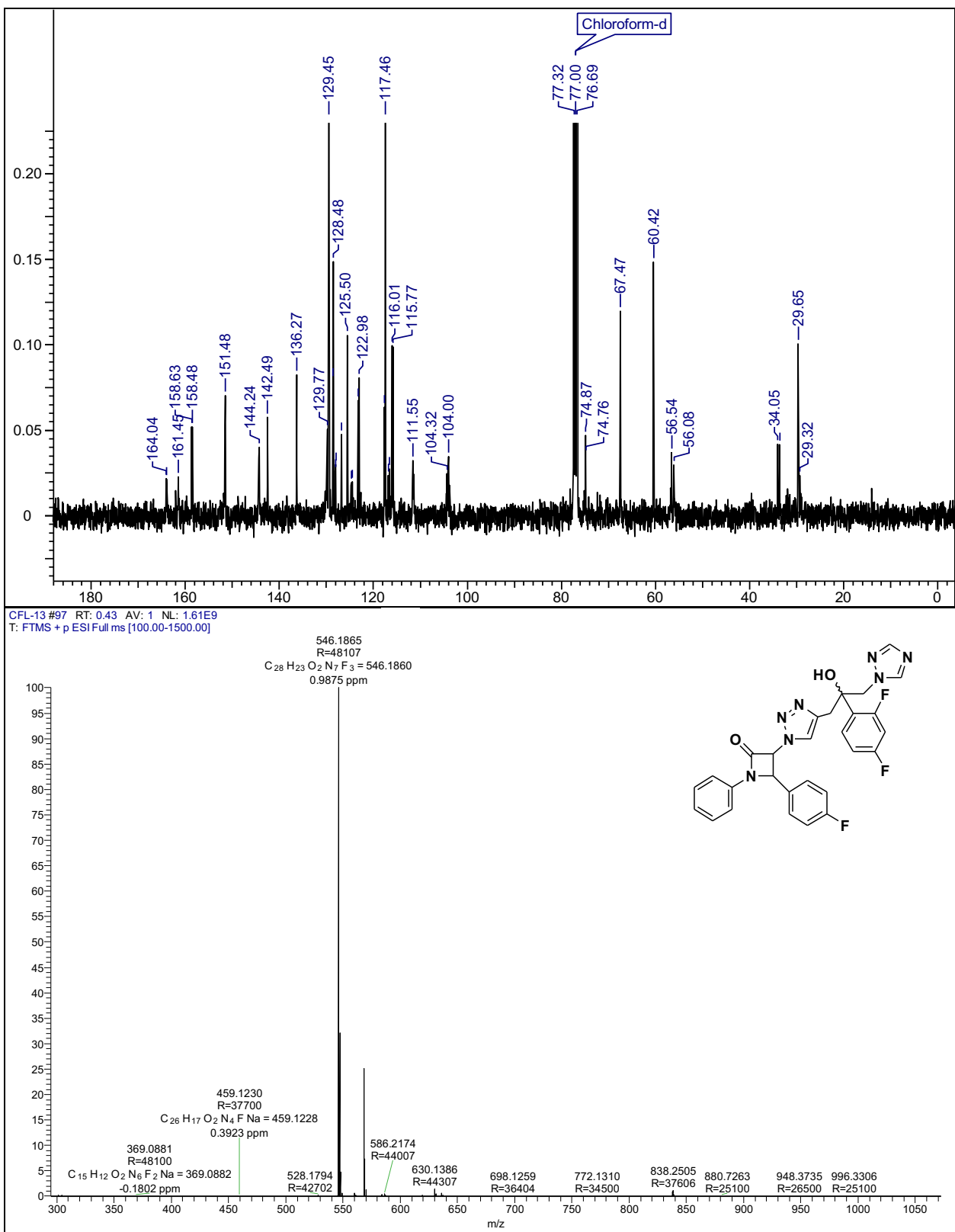


*3-(4-(2-(2,4-difluorophenyl)-2-hydroxy-3-(1*H*-1,2,4-triazol-1-yl)propyl)-1*H*-1,2,3-triazol-1-yl)-4-(4-fluorophenyl)-1-phenylazetidin-2-one; **12l**.* Yield: 90%; semi-solid; IR (CHCl₃, cm⁻¹) 3415, 1761; ¹H NMR (CDCl₃, 400 MHz) δ 7.96-8.0 (m, 1H), 7.79-7.83 (m, 1H), 7.32-7.40 (m, 5H, Ar-H), 7.20-7.25 (m, 2H, Ar-H), 7.09-7.18 (m, 2H, Ar-H), 6.78-6.87 (m, 2H), 6.69-6.73 (m, 2H), 6.24-6.31 (m, 1H), 5.59-5.63 (m, 1H), 5.11-5.22 (m, 1H), 4.54-4.61 (m, 1H), 3.88-4.20 (m, 1H), 3.03-3.26 (m, 2H); ¹³C NMR (CDCl₃, 50 MHz) δ 164.0, 163.9, 161.4, 158.6, 158.4, 151.4, 144.2, 142.4, 136.2, 129.7, 129.4, 128.4, 125.5, 122.9, 117.4, 116.0, 115.7, 111.5, 104.3, 104.0, 74.92, 74.8, 74.7, 67.4, 60.4, 56.5, 34.0, 33.6, 29.3. ESI-MS (m/z): 546.18 [M+H]⁺; HRMS (ESI-qTOF): calcd for C₂₈H₂₃F₃N₇O₂ [M+H]⁺, 546.1860: found: 546.1865.

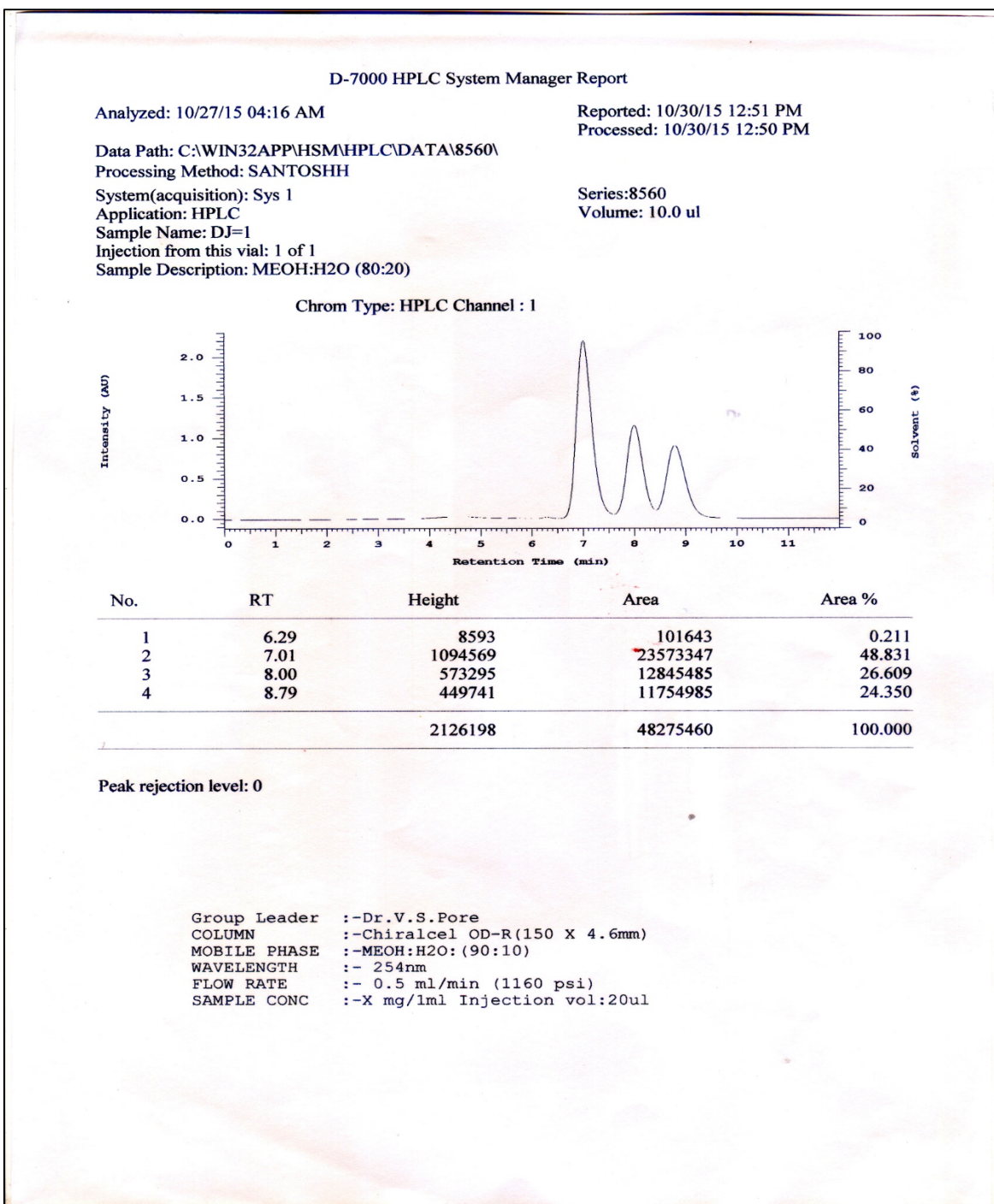
12l



12l



HPLC Data of compound 12j



Reference

- 1 R.A. Friesner et. al, *J. Med. Chem.*, 2006, **49**, 6177.
- 2 T. A. Halgren et.al., *J. Med. Chem.*, 2004, **47**, 1750.
- 3 R.A. Friesner et. al, *J. Med. Chem.*, 2004, **47**, 1739.
- 4 T. Mosmann, *J. Immunol. Methods*, 1983, **65**, 55.
- 5 G. Ciapetti, E. Cenni, L. Pratelli, A. Pizzoferrato, *Biomaterials*, 1993, **14**, 359.